Monte Calro simulation of electrolyte solution dynamics

（電解質溶液の動的挙動に関するモンテカルロシミュレーション）

Masafumi Yoshida

Monte Calro simulation of electrolyte solution dynamics

Masafumi Yoshida

This thesis is submitted to The University of Tokyo as a doctoral dissertation

Contents

1. Introduction

Polyelectrolytes are molecules having many ionizable groups. They dissociate in solution into polyions and a large number of counterions. Biochemical substances such as proteins and nucleic acids are examples of natural polyelectrolytes. Their peculiar behavior in solution has attracted many researchers in the field of physical chemistry of electrolytes and polymers.

Electric birefringence and electric dichroism are techniques now widely used to study dynamic properties of polymers in solution. In these experiment, an electric field is applied to the solution and its optical response (birefringence or dichroism) is recorded. By analyzing the electro-optical transient one can determine relaxation times of the molecular motion undergone by the polymers.

The theoretical description of response of polyelectrolyte molecules in solution to applied electric field is an extremely complex and difficult problem even if simple models are assumed for the geometry of the polyions. This is because Coulombic forces among charges and hydrodynamic interactions among diffusing particles are both long-range and there are involved many field: concentrations of small ions, the electrical potential, and solvent viscosity, to be determined as functions of space and time which are coupled with each other through essentially nonlinear equation. Consequently in many theoretical studies recourse has been had to somewhat ad hoc approximations such that counterions are classified into " free " and " bound " ions, only the latter contributing to the induced moment whose interaction with the applied electric field causes orientation of the polyions along the field.

In this thesis the author used the Metropolis Monte Carlo (MC) simulation[1] method to approach the problem in a practical way. The method is one of the standard simulation techniques now widely used to study the properties of fluids which are composed of many interacting

molecules. It was introduced by Metropolis et al. as a method suited for electronic computers to carry out a many-dimensional integral over the configuration space. In the scheme a Markov chain of states of the liquid is constructed and the elements of transition matrix is devised to generate a trajectory in phase space which samples a representative portion from the canonical ensemble. The method has been conventionally regarded as applicable to the study of equilibrium properties. To obtain the dynamic properties, a different technique, molecular dynamics, has been required. In Chapter 2, however, the author shows[2,3] that the Metropolis Monte Carlo method when applied to part of the degrees of freedom of a system, e.g. colloidal particles embedded in a solvent continuum, turns into a simulation procedure of the Brownian motion of the solute particles.

Main advantage of the Monte Carlo simulation is the speed of calculation. In this method, only the behavior of solute ions is calculated, and the solvent is considered as a continuum. Then, the MC simulation is more than 1000 times faster than the molecular dynamics (MD) simulation. As shown in Chapter 2 , MC simulation can reproduce phenomena whose relaxation times are longer than 10^{-9} second. The Langevin dynamics (LD) simulation is carried out by numerically solving the Langevin equation. Since the MC simulation in this thesis is based on the Langevin equation, the LD method is almost equivalent to the MC method. However its algorithm is a little complicated in the case of considering discontinuous potentials, for example collision of the ions. Another possible approach for obtaining the behavior of solute ions is numerical calculation of the diffusion equation. However, since it is a multivariable differential equation, some additional approximation have been used.

The method thus provides a powerful tool for investigating the dynamics of polymers whose motion is usually described by diffusion equation.

In the greater part of the thesis, the author describes the applications of the method to polyelectrolyte solutions. Simulations carried out step by step in order to clarify the mechanism of orientation of polyelectrolytes in an external electric field (Fig. 1) . First in Section 3.2 diffusion of

simple ions in studied for NaCl solutions. Dynamics in NaCl solution has been studied by other simulation methods[4,5] , and the diffusion coefficients have been exprimentally measured[6]. In Section 3.3 an algorithm is devised to simulate rotational Brownian motion of a rod-like polyion. In Section 3.4 polarization of the counterion atmosphere around a fixed polyion is simulated. This is the first attempt to reproduce the polarization of polyelectrolytes by computer simulation[7,8] , while static properties have been studied by MC simulation[9]. Finally in Section 3.5 simulation of coupled rotational and ion atmosphere dynamics of a polyelectrolyte is attempted.

While extensive calculations with more realistic models may be needed for comparison with experiment, the method developed in this thesis is expected to be most useful for studying dynamics of polyelectrolyte solution.

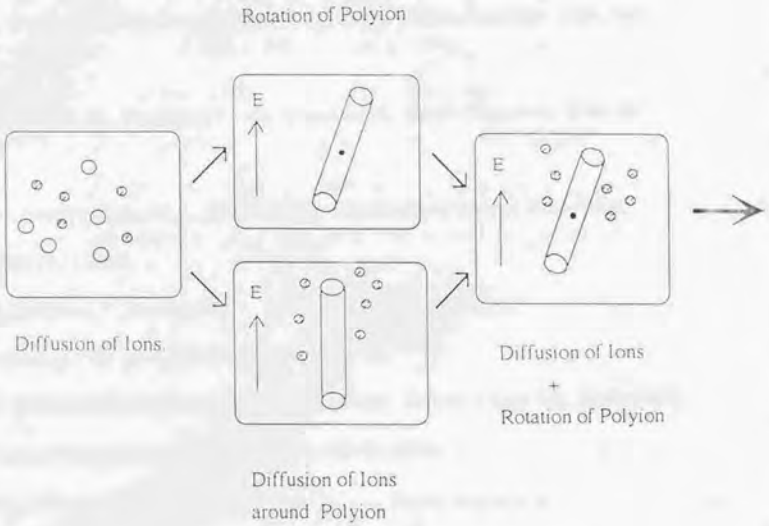

Fig.1 Simulations were carried out step by step in this thesis: diffusion of counterions in Section 3.2, rotation of polyion in Section 3.3, diffusion of counterions around polyion in Section 3.4, and diffusion of counterions + rotation of polyion in Section 3.5.

References

1) Metropolis, N., Rosenbush, A. W., Rosenbush, M. N, Teller, A. H., and Teller, E. *J. Chem. Phys.* **21** (1953) 1987

2) Kikuchi,K., Yoshida,M., Maekawa,T., and Watanabe,H. *Chem.Phys.Lett.* **185**, 335 (1991)

3) Kikuchi,K., Yoshida,M., Maekawa,T., and Watanabe,H. *Chem.Phys.Lett.* **196**, 57 (1992)

4) Wood, D. M. and Friedman, H. L. *Zeitschrift fur Physikalische Chemie Neue Folge*, bd. 155, S.121-132 (1987)

5) Turq, P and Lantelme, F *J.Chem.Phys.* , **66**, 3039 (1977)

6) Mills,R *Reviews of Pure and Applied Chemistry*

7) Yoshida,M.,Kikuchi,K., Maekawa,T., and Watanabe,H. *J.Phys. Chem.* **96**, 2365 (1992)

8) Yoshida,M., and Kikuchi,K.*J.Phys. Chem.* **98**, 10303(1994)

9) Vlachy et al. J. Chem. Phys., **76**, 15 (1982)

2. Method

In this thesis, the behavior of the solute ions was focused on, and the behavior and structure of the solvent were not discussed. Then, the motion of the ions was considered as the Brownian motion which obeys the Langevin equation. In Section 2.1, the Brownian motion of solute ions was discussed . The required accuracy of simulation was the same as the diffusion equation, by which various phenomena in colloidal and polymer solutions have been described. In Section 2.2, it was shown that the Metropolis Monte Carlo method is one of such simulation method, and parameters and errors were discussed.

2.1 Brownian motion of solute ions

In this section, we discuss the motion of the solute ions in electrolyte solutions. The Langevin equation for solute ions is derived [1] , and the mean displacement $< \Delta x >$ and the mean square displacement $< \Delta x^2 >$ are calculated for comparison with those by the Monte Carlo method.

2.1.1 Langevin equation

We consider a electrolyte solution which consists of solute ions (ex. Na^+) and solvent molecules (ex. H_2O). The motion of i th solute ion obeys the following equation of motion:

$$m \ddot{x}_i = \sum_j F_1 (x_i , x_j) + \sum_k F_2 (x_i , x_k) + F_3 \qquad (1)$$

where $F_1(x_i, x_j)$ is the force from the j th solute ions , $F_2(x_i, x_j)$ is that from the k th solvent molecule, and F_3 is the external force. In eq(1), we assume that the solution is dilute so that the effect of the solvent molecules is independent of the other solute ions. Furthermore, assuming that the effect of the solvent molecules is independent of the position x_i , eq(1) is written as:

$$m\ddot{x}_i = \sum_j F_1(x_i, x_j) + F_3 - \zeta \dot{x} + R(t) \tag{2}$$

where, $\zeta \dot{x}$ is a frictional force and $R(t)$ is the random force. These two terms come from the interactions between the solute ion and the surrounding solvent molecules. The random force $R(t)$ is assumed to have the following statistical properties [1] :

$$< R(t_1) > = 0 \tag{3}$$

$$< R(t_1)R(t_2) > = m^2 \varepsilon \delta(t_1 - t_2) \tag{4}$$

where $<\ >$ represents the average over the solute ions, δ is the Kronecker delta function.

We assume that the force from the other solute ion $F_1(x_i, x_j)$ and the external force F_3 are given by the potential U .

$$\frac{\partial U}{\partial x_i} = -\sum_j F_1(x_i, x_j) - F_3 \tag{5}$$

From now on, we omit the suffix i , and assume U can be expanded as :

$$U(x) = U(x_0) + \left(\frac{\partial U}{\partial x}\right)_{x0} (x - x_0) + \frac{1}{2}\left(\frac{\partial^2 U}{\partial x^2}\right)_{x0} (x - x_0)^2 + \cdots \tag{6}$$

Then eq (2) becomes:

$$m\ddot{x} = -C_1 - C_2(x - x_0) - \zeta \dot{x} + R(t) \tag{7}$$

where,

$$C_1 = \left(\frac{\partial U}{\partial x}\right)_{x0} \qquad C_2 = \left(\frac{\partial^2 U}{\partial x^2}\right)_{x0} \tag{8}$$

Eq(7) is also written as:

$$\ddot{x} = -c_1 - c_2(x - x_0) - \beta \dot{x} + \lambda(t) \tag{8}$$

where,

$$\lambda(t) = R(t) / m \,,\ \beta = \zeta / m \,,\ c_1 = C_1 / m \,,\ c_2 = C_2 / m \tag{9}$$

In aqueous solutions, the frictional force for the solute ion is so large that its velocity becomes equilibrium soon. For example, ζ of Na^+ ion is 3×10^{-12} kg/s and its relaxation time β^{-1} is estimated to be larger than the order of 10^{-14} second. Therefore, the left hand side of eq(8) is almost always zero:

$$0 = -c_1 - c_2(x - x_0) - \beta \dot{x} + \lambda(t) \tag{10}$$

This assumption has been called as the Smolchowski level approximation. The ordinary diffusion equation is also based on this assumption. The formal solution of eq(10) is

obtained as:

$$x = x_0 e^{-\frac{c_2}{\beta}t} + e^{-\frac{c_2}{\beta}t} \int_0^t \beta^{-1} e^{\frac{c_2}{\beta}t_1} (\lambda(t_1) - c_1 - c_2 x_0) \, d t_1$$

$$= x_0 + e^{-\frac{c_2}{\beta}t} \int_0^t \beta^{-1} e^{\frac{c_2}{\beta}t_1} (\lambda(t_1) - c_1) \, d t_1 \qquad (11)$$

Since $\lambda(t)$ is a random variable and only its stochastic properties eq(3) and eq(4) are given, we can not reduce eq(11) any more.

2.1.2 Expected values of displacement

The Langevin equation includes the random variable $\lambda(t)$. Then only the statistical values such as the mean displacement can be obtained from the Langevin equation. The mean displacement $< \Delta x >$ and the mean square displacement $< \Delta x^2 >$ are important, because the diffusion equation is defined as

$$\frac{\partial}{\partial t} P(x,t) = \left(-\frac{\partial}{\partial x} < \Delta x > + \frac{1}{2} \frac{\partial^2}{\partial x^2} < \Delta x^2 > \right) P(x,t) \tag{12}$$

Mean displacement $< \Delta x >$

We consider the displacement of the solute ion Δx in a period of Δt. The average of Δx over the solute ions is written as:

$$\begin{aligned} < \Delta x > &= < x - x_0 > \\ &= < e^{-\frac{c_2}{\beta}\Delta t} \int_0^{\Delta t} \beta^{-1} e^{\frac{c_2}{\beta} t_1} (\lambda(t_1) - c_1) \, d t_1 > \\ &= e^{-\frac{c_2}{\beta}\Delta t} \int_0^{\Delta t} \beta^{-1} e^{\frac{c_2}{\beta} t_1} (< \lambda(t_1) > - c_1) \, d t_1 \end{aligned} \tag{13}$$

Since $< \lambda(t) > = 0$, it becomes:

$$< \Delta x > = -\frac{C_1}{C_2} (1 - e^{-\frac{c_2}{\beta}\Delta t}) \tag{14}$$

Expanding the exponent on Δt, it becomes:

$$< \Delta x > = -\frac{C_1}{\beta} \Delta t + o(\Delta t) \tag{15}$$

Considering eq(8), $< \Delta x >$ is written as:

$$< \Delta x > = -\frac{1}{m\beta} \left(\frac{\partial U}{\partial x} \right)_{x_0} \Delta t + o(\Delta t) \tag{16}$$

Mean square displacement $< (\Delta x)^2 >$

The average of Δx^2 in a period of Δt is written as:

$$< \Delta x^2 > = < (x - x_0)^2 >$$

$$= < e^{-\frac{2c_2}{\beta} \Delta t} \int_0^{\Delta t} \int_0^{\Delta t} \beta^{-2} e^{\frac{c_2}{\beta}(t_1 + t_2)} (\lambda(t_1) - c_1)(\lambda(t_2) - c_1)\, dt_1 dt_2 >$$

$$= < e^{-\frac{2c_2}{\beta} \Delta t} \int_0^{\Delta t} \int_0^{\Delta t} \beta^{-2} e^{\frac{c_2}{\beta}(t_1 + t_2)} \{ <\lambda(t_1)\lambda(t_2)> - c_1 <\lambda(t_1)> - c_1 <\lambda(t_2)> + c_1^2 \}\, dt_1 dt_2 \tag{17}$$

Since $< \lambda(t) > = 0$ and $< \lambda(t_1)\, \lambda(t_2) > = \varepsilon\, \delta(t_1 - t_2)$, it becomes :

$$<\Delta x^2> = \frac{\varepsilon}{2c_2\beta}\left(1 - e^{-\frac{2c_2}{\beta}\Delta t}\right) + \frac{c_1^2}{c_2^2}\left(1 - 2e^{-\frac{c_2}{\beta}\Delta t} + e^{-\frac{2c_2}{\beta}\Delta t}\right) \qquad (18)$$

Expanding the exponent on Δt, eq(18) is written as:

$$<(\Delta x)^2> = \frac{\varepsilon}{\beta^2}\Delta t + o(\Delta t) \qquad (19)$$

2.1.3 Relations to Temperature and Diffusion coefficient

The Langevin equation includes the microscopic parameters, ε and β. In order to obtain their relation to the macroscopic quantities, temperature and diffusion coefficient, we consider the motion of an solute ion in infinite dilute solutions. The Langevin equation of such an ion is:

$$\ddot{x} = -\beta \dot{x} + \lambda(t) \tag{20}$$

Temperature

From eq(20), the velocity $v = \dot{x}$ of the ion is obtained as:

$$v = v_0 e^{-\beta t} + e^{-\beta t} \int_0^t e^{\beta t_1} \lambda(t_1)\, d t_1 \tag{21}$$

Then v^2 is :

$$v^2 = v_0^2 e^{-2\beta t} + 2 v_0 e^{-\beta t} \int_0^t e^{2\beta t_1} \lambda(t_1)\, d t_1 + e^{-2\beta t} \int_0^t \int_0^t e^{\beta t_1} e^{\beta t_2} \lambda(t_1) \lambda(t_2)\, d t_1\, d t_2 \tag{22}$$

The average of v^2 is obtained by similar calculations in 1.1.2 :

$$\langle v^2 \rangle = v_0 e^{-2\beta t} + \frac{\varepsilon}{2\beta}(1 - e^{-2\beta t}) \tag{23}$$

In the limit of $t \to \infty$,

$$< v^2 > \rightarrow \frac{\varepsilon}{2\beta} \tag{24}$$

Therefore, the average of the kinetic energy of the ion is :

$$\left\langle \frac{1}{2} m v^2 \right\rangle = \frac{1}{2} m < v^2 > = \frac{m \varepsilon}{4 \beta} \tag{25}$$

Considering the equi-partition law,

$$\left\langle \frac{1}{2} m v^2 \right\rangle = \frac{1}{2} k_B T \tag{26}$$

Therefore, the ratio of β and ε is expressed by the temperature T.

$$\frac{\varepsilon}{\beta} = 2 \frac{k_B T}{m} \tag{27}$$

Diffusion coefficient

There should be another equation for ε and β in order to determine the absolute values of them. Such a equation is obtained by considering the diffusion coefficient. From eq(21), the displacement Δx of the solute ion in a period of Δt is obtained:

$$\Delta x = x - x_0 = \frac{v_0}{\beta} (1 - e^{-\beta t}) + \int_0^t e^{-\beta t_2} \int_0^{t_2} e^{\beta t_1} \lambda (t_1) \, d t_1 \, d t_2 \tag{28}$$

Then the mean square displacement is :

$$<(\Delta x)^2> = \frac{v_0^2}{\beta^2}(1-e^{-\beta t})^2 + \frac{\varepsilon}{\beta^2}\left\{t + \frac{1}{2\beta}(1-e^{-2\beta t}) - \frac{2}{\beta}(1-e^{-\beta t})\right\} \tag{29}$$

where, the properties of the random force, $<\lambda(t)> = 0$ and $<\lambda(t_1)\lambda(t_2)> = \varepsilon\,\delta(t_1-t_2)$, are considered. In the limit of $t \to \infty$,

$$<x^2> \to \frac{\varepsilon}{\beta^2} t \tag{30}$$

In the experimental study, the diffusion coefficient in one dimension is defined as:

$$D = \lim_{\Delta t \to \infty} \frac{<(x(t+\Delta t) - x(t))^2>}{2\Delta t} \tag{31}$$

Therefore, the parameters β and ε are found to be related to the experimental diffusion coefficient.

$$\frac{\varepsilon}{\beta^2} = 2D \tag{32}$$

The diffusion coefficient D is obtained by the experiments. It should be noted that D is the value of the infinite dilute solution, because Eq(20) is the equation of motion for the ion in the infinite dilute solutions.

2.1.4 Discussion

The two parameters are expressed in terms of temperature T and the diffusion coefficient D.

$$\beta = \frac{k_B T}{m^2 D} \quad , \quad \varepsilon = \frac{2 (k_B T)^2}{m D} \tag{33}$$

Then, the mean value $< \Delta x >$ and $< \Delta x^2 >$ become:

$$< \Delta x > = - \frac{D}{k_B T} \left(\frac{\partial U}{\partial x} \right)_{x_0} \Delta t \ + o(\Delta t) \tag{34}$$

$$< \Delta x^2 > = 2 D \Delta t \ + o(\Delta t) \tag{35}$$

In this thesis, the author requires a simulation method which reproduce the motion of solute ions with the same accuracy as the diffusion equation. In view of the fact that diffusion equation neglects higher other than Δt , we can use a simulation method which satisfies eq(35) and eq(36) . As discussed in Section 2.2, Metropolis Monte Carlo method is one of such simulation methods.

References

1) Wax, N. ed. *Noise and stochastic Processes (Dover publications, New York, 195-)*

2.2 Monte Carlo method

The simulations in this work were carried out by the Metropolis Monte Carlo method[1]. Advantage of this method is the speed of calculation, and it can be used for phenomena whose duration is longer than 10^{-8} second as shown in Chapter 3 . This method has been widely used for the study of fluids and solutions [2]. However, the Metropolis scheme is originally developed for calculating the average over the configuration space [3,4]. Then the dynamics in solutions have not been studied by this method. In this section, we show that the Monte Carlo method can be applied to the non-equilibrium system [5,6].

2.2.1 Metropolis scheme

Fig 2-2-1 shows the main part of the Metropolis scheme. The Monte Carlo time Δt should not be considered as the real time unless the d_{max} is small enough. If N particles system is considered, the Metropolis scheme can be applied to 3N dimensional vector.

Maximum trial displacement d_{max}

In order to study the dynamics in solutions, the maximum trial displacement d_{max} should be chosen :

$$d_{max}{}^2 = 6\,D\,\Delta t \qquad (1)$$

where, D is the diffusion coefficient of the solute ions in infinite dilute solutions. Table 2-2-1 shows the relation of d_{max} between Δt for aqueous Na^+ ions. As discussed 2.3, the accuracy of the simulation depends on Δt . In the case of dilute electrolyte solutions, Δt is required to be the order of 10^{-12} second. Then, Δt is set to be 1.25 ps for the

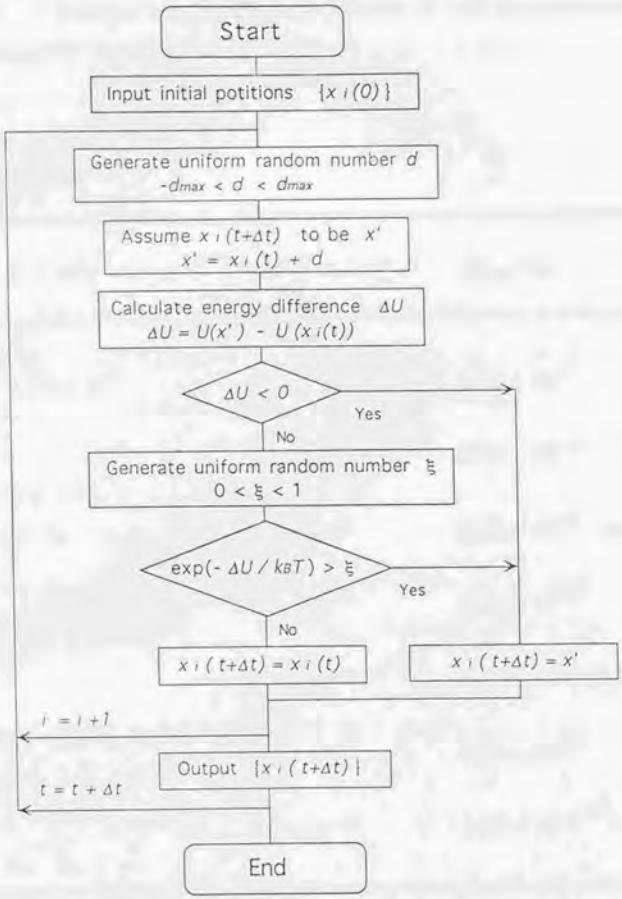

Fig.2-2-1 Metropolis Monte Carlo schme for the Brownian motion. $x_i(t)$: position of the i th particle. Δt : time interval corresponding to one step if d_{max} is chosen small enough .

Table 2-2-1 Relation between the time interval Δt and the maximum trial displacement d_{max} for the aqueous Na^+ ion.

D / m^2s^{-1}	Δt / s	d_{max} / m
1.33×10^{-9}	1.0×10^{-9}	2.82×10^{-9}
	1.0×10^{-10}	8.93×10^{-10}
	1.0×10^{-11}	2.82×10^{-10}
	1.0×10^{-12}	8.93×10^{-11}
	1.0×10^{-13}	2.82×10^{-11}
	1.0×10^{-14}	8.93×10^{-12}
	1.0×10^{-15}	2.82×10^{-12}

Δt is required to be the order of 10^{-12} second. Then, Δt is set to be 1.25 ps for the almost simulations in this work. Table2-2-2 shows the values of d_{max} for the several aqueous ions. If the solution consists of more than one spices of ions, d_{max} should vary for ion spices.

Boundary condition

The periodic boundary condition is always used. However, if a ion goes out of the unit cell, the energy difference ΔU should be calculated before the ion is brought back to the unit cell. Otherwise, the stationary flow of the ions due to the external field can not be reproduced. In principle, the image ions in the surrounding 26 replica cells are considered for calculating the energy difference ΔU .

Random numbers

The simulations in this work needs more than 10^8 random numbers. The congruential method were used to generate the random numbers. In the case of using the vector computer S3800 at The University of Tokyo, the subroutine developed for it were used. The uniformity of the random numbers were always checked , however the long range correlations of the random numbers were difficult to be checked.

Table 2-2-2 The maximum trial displacement d_{max} of the aqueous ions for the simulation of Δt = 1ps .

Δt / s	*ion*	D / $10^{-9}m^2s^{-1}$	d_{max} / nm
1.0×10^{-12}	L_i^+	1.03	0.0692
	N_a^+	1.33	0.0893
	K^+	1.96	0.1315
	C_a^{2+}	1.57	0.1054
	Cl^-	2.03	0.1363
	F^-	1.45	0.0974

2.2.2 Application to dynamics

The Metropolis Monte Carlo method has been believed to be applicable to only the steady state. If it were true, the dynamic phenomena in electrolyte solutions could not be studied by this method. However, the Metropolis Monte Carlo method was found to be applied to the dynamics. In this section, we show that the mean values, $< \Delta x >$ and $< (\Delta x)^2 >$, from the Monte Carlo simulation agree with those from the Langevin equation in the order of Δt. .

Mean displacement $< \Delta x >$

The mean displacement in one Monte Carlo step ,$< \Delta x >$, is written as:

$$<\Delta x> = \int_{\Delta U<0} d_{max}\,\xi\,\pi(\xi)\,d\xi + \int_{\Delta U>0} d_{max}\,\xi\,\pi(\xi)\,exp\left(-\frac{\Delta U}{k_B T}\right)d\xi \qquad (2)$$

where, ξ is the uniform random variable ($-1 < \xi < 1$), $\pi(\xi)$ is the probability density of ξ ($\pi(\xi) = 1/2$) . The first term is the integral over the ξ corresponding to $\Delta U < 0$ and the second is that to $\Delta U > 0$.

If d_{max} is small enough for $\Delta U / k_B T << 1$, the exponent in eq(2) can be expanded as :

$$exp\left(-\frac{\Delta U}{k_B T}\right) = 1 - \frac{\Delta U}{k_B T} + \frac{1}{2}\left(\frac{\Delta U}{k_B T}\right)^2 + \ldots \qquad (3)$$

Then, eq(2) becomes :

$$< \Delta x > = \int_{\Delta U < 0} d_{max}\, \xi\, \pi\,(\xi)\, d\,\xi + \int_{\Delta U > 0} d_{max}\, \xi\, \pi\,(\xi)\, d\,\xi$$

$$- \int_{\Delta U > 0} d_{max}\, \xi\, \pi\,(\xi)\, \frac{\Delta U}{k_B T}\, d\,\xi + o\,(\Delta U^2) \qquad (4)$$

The first two terms cancel each other because $\pi(\xi)$ is constant:

$$< \Delta x > = - \int_{\Delta U > 0} d_{max}\, \xi\, \pi\,(\xi)\, \frac{\Delta U}{k_B T}\, d\,\xi + o\,(\Delta U^2) \qquad (5)$$

Expanding ΔU as:

$$\Delta U = \left(\frac{\partial U}{\partial x}\right) d_{max}\, \xi + \frac{1}{2}\left(\frac{\partial^2 U}{\partial x^2}\right) d_{max}^2\, \xi^2 + \qquad (6)$$

Then,

$$< \Delta x > = - \int_{\Delta U > 0} \frac{1}{k_B T}\left(\frac{\partial U}{\partial x}\right) d_{max}^2\, \xi^2\, \pi\,(\xi)\, d\,\xi + o\,(d_{max}^2) \qquad (7)$$

Since ξ is uniform and $\pi(\xi)$ is constant , eq(7) becomes:

$$< \Delta x > = - \frac{1}{6\, k_B T}\left(\frac{\partial U}{\partial x}\right) d_{max}^2 + o\,(d_{max}^2) \qquad (8)$$

Mean square displacement $< (\Delta x)^2 >$

The mean square displacement $< (\Delta x)^2 >$ is written as:

$$<\Delta x^2> = \int_{\Delta U<0} d_{max}^2 \xi^2 \pi(\xi) d\xi + \int_{\Delta U>0} d_{max}^2 \xi^2 \pi(\xi) exp\left(-\frac{\Delta U}{k_B T}\right) d\xi \tag{9}$$

Expanding the exponent as discussed above, it becomes:

$$<(\Delta x)^2> = \int_{\Delta U<0} d_{max}^2 \xi^2 \pi(\xi) d\xi + \int_{\Delta U>0} d_{max}^2 \xi^2 \pi(\xi) d\xi$$

$$- \int_{\Delta U>0} d_{max}^2 \xi^2 \pi(\xi) \frac{\Delta U}{k_B T} d\xi + o(\Delta U^2) \tag{10}$$

Since $\pi(\xi) = 1/2$, the first two terms make $d_{max}^2 / 3$. The third term is higher order than d_{max}^2. Therefore, $< (\Delta x)^2 >$ in one Monte Carlo step is obtained:

$$<(\Delta x)^2> = \frac{d_{max}^2}{3} + o(d_{max}^2) \tag{11}$$

Comparison with Langevin equation

Table 2-2-3 shows $< \Delta x >$ and $< (\Delta x)^2 >$ from both the Monte Carlo method and the Langevin equation. It is seen that $< \Delta x >$ and $< (\Delta x)^2 >$ by both method agree with each

Table 2-2-3 The mean displacement $< \Delta x >$ and the mean square displacement $< \Delta x^2 >$ of the Brownian motion. The relation $d_{max}^2 = 6D\Delta t$ holds.

	Monte Carlo Simulation	Langevin equation (Smolchowski level)
$< \Delta x >$	$-\frac{1}{6 k_B T}\left(\frac{\partial U}{\partial x}\right) d_{max}^2 + o(d_{max}^2)$	$-\frac{D}{k_B T}\left(\frac{\partial U}{\partial x}\right)\Delta t + o(\Delta t)$
$< (\Delta x)^2 >$	$\frac{1}{3} d_{max}^2 + o(d_{max}^2)$	$2 D \Delta t + o(\Delta t)$

other , if the higher orders than $d_{max}{}^2$ and Δt are neglected, and if the following relation holds:

$$d_{max}{}^2 = 6\,D\,\Delta t \tag{12}$$

That is, if d_{max} is determined by eq(12) , the Monte Carlo simulation can reproduce $< \Delta x >$ and $< (\Delta x)^2 >$ in the order of Δt . Furthermore, this means that the Monte Carlo simulation is equivalent to the diffusion equation:

$$\frac{\partial}{\partial t} P(x, t) = D \left(\frac{\partial}{\partial x^2} + \frac{\partial}{\partial x} \frac{f}{k_B T} \right) P(x, t) \tag{13}$$

because eq(13) comes from eq(14) and the higher order than t^2 are neglected in the derivation of eq(14) :

$$\frac{\partial}{\partial t} P(x, t) = \left(- \frac{\partial}{\partial x} < \Delta x > + \frac{1}{2} \frac{\partial^2}{\partial x^2} < \Delta x^2 > \right) P(x, t) \tag{14}$$

2.2.3 Estimation of the error

In this section, $< \Delta x >$ and $< \Delta x^2 >$ are considered up to the order of Δt^2. By using these expressions, the diversion of the results of the Monte Carlo method from the analytical results of the Langevin equation is discussed. Then, the error of the simulation of the polyelectrolyte solutions is found to be sufficiently small at $\Delta t = 1.25$ ps.

$< \Delta x >$ and $< \Delta x^2 >$ up to the order of Δt^2

Considering the higher order than Δt of eq(2) and eq(9), $< \Delta x >$ and $< \Delta x^2 >$ of the Monte Carlo method are written as:

$$< \Delta x > = - \frac{D}{k_B T} \left(\frac{\partial U}{\partial x} \right)_{x_0} \Delta t + \frac{(6D)^{3/2}}{16 k_B^2 T^2} \left(\frac{\partial U}{\partial x} \right)_{x_0}^2 \Delta t^{3/2}$$

$$- \frac{(6D)^{3/2}}{16 k_B T} \left(\frac{\partial^2 U}{\partial x^2} \right)_{x_0} \Delta t^{3/2} + \frac{9 D^2}{5 k_B^2 T^2} \left(\frac{\partial^2 U}{\partial x^2} \right)_{x_0} \left(\frac{\partial U}{\partial x} \right)_{x_0} \Delta t^2$$

$$+ o(\Delta t^2) \qquad (15)$$

$$< \Delta x^2 > = 2 D \Delta t - \frac{(6D)^{3/2}}{8 k_B T} \left(\frac{\partial U}{\partial x} \right)_{x_0} \Delta t^{3/2}$$

$$+ \frac{9 D^2}{5 k_B^2 T^2} \left(\frac{\partial U}{\partial x} \right)_{x_0}^2 \Delta t^2 - \frac{9 D^2}{5 k_B T} \left(\frac{\partial^2 U}{\partial x^2} \right)_{x_0} \Delta t^2 + o(\Delta t^2) \quad (16)$$

Considering the higher order than Δt of eq(14) and eq(18) in 2.1, $< \Delta x >$ and $< \Delta x^2 >$ from the Langevin equation are written as:

$$< \Delta x > = - \frac{D}{k_B T} \left(\frac{\partial U}{\partial x} \right)_{x_0} \Delta t + \frac{D^2}{2 k_B^2 T^2} \left(\frac{\partial^2 U}{\partial x^2} \right)_{x_0} \left(\frac{\partial U}{\partial x} \right)_{x_0} \Delta t^2 + o(\Delta t^2) \quad (17)$$

$$< \Delta x^2 > = 2 D \Delta t + \frac{D^2}{k_B^2 T^2} \left(\frac{\partial U}{\partial x} \right)_{x_0}^2 \Delta t^2 - \frac{2 D^2}{k_B T} \left(\frac{\partial^2 U}{\partial x^2} \right)_{x_0} \Delta t^2 + o(\Delta t^2) \quad (18)$$

Error under external fields.

Fig.2-2-2 shows the error of $< \Delta x >$ for the aqueous Na^+ ion under an uniform external field. The field strength E = 10.6 MV / m is almost upper limit of the experiments [8]. Fig.2-2-3 shows the error of $< \Delta x^2 >$. In this case, the error of the simulation comes from the term of $\Delta t^{3/2}$ only, as shown in Fig.2-2-2 and Fig.2-2-3. If Δt = 1.25 ps, the error of the simulation is expected to be below 1 %.

Error in Coulombic potential

Fig.2-2-4 shows the error of $< \Delta x^2 >$ for the aqueous Na^+ ion near a negative charge (ex. Cl^-). In the simulation of the polyelectrolyte solutions, the error is expected to be below 2 % for Δt = 1.25 ps, because the minimum distance between Na^+ and the negative charge of the polyion is 1 nm. However in the simulation of NaCl solutions, the error is 10 % at worst, because the minimum distance between Na^+ and Cl^- is about 0.5 nm.

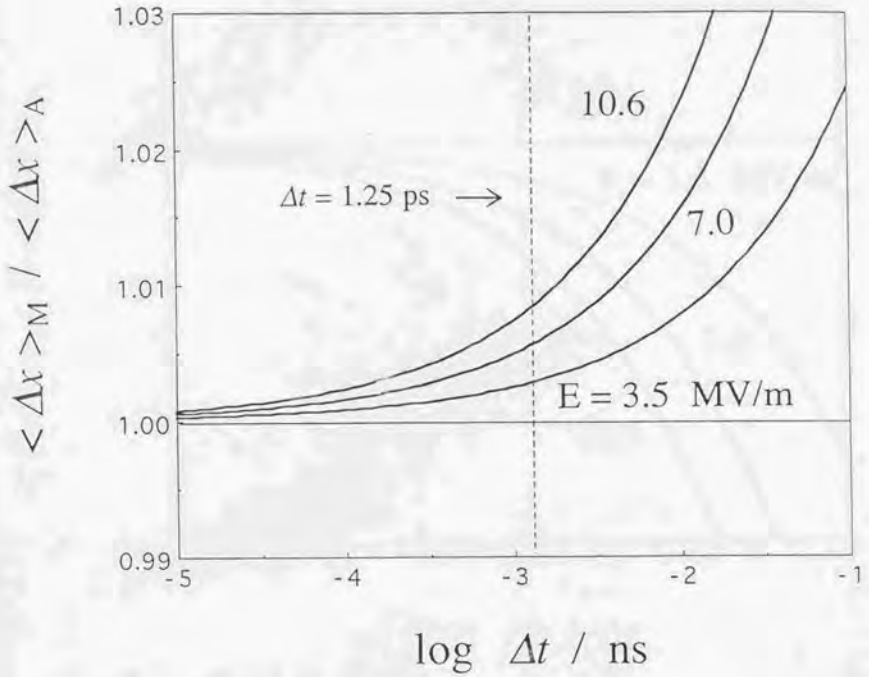

Fig.2-2-2 Δt dependence of the accuracy of the Monte Carlo simulation of the Na^+ ion under the electric field E . $< \Delta x >_M$ and $< \Delta x >_A$ are the mean displacements in Δt . $< \Delta x >_M$: Monte Carlo , $< \Delta x >_A$: analytical result. T = 298K.

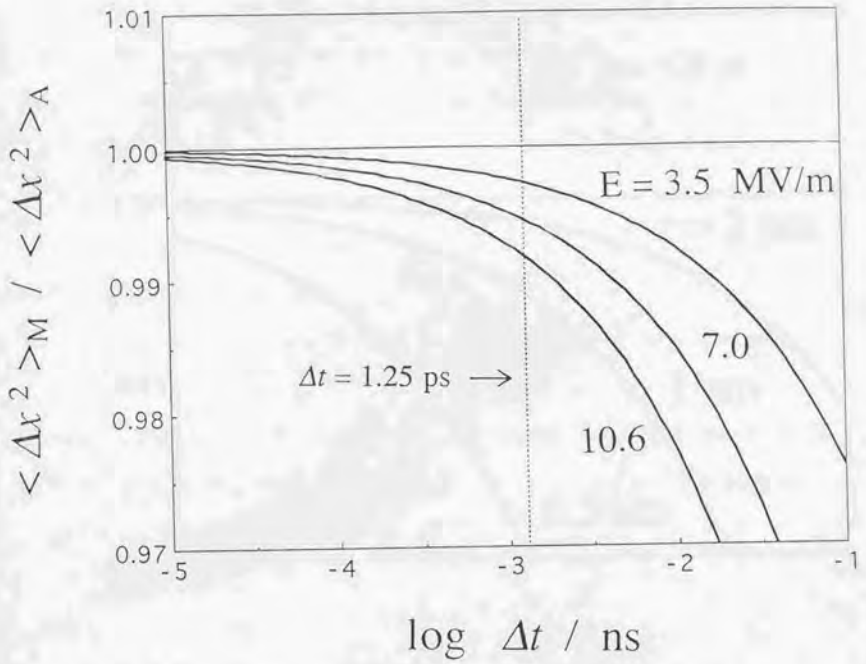

Fig.2-2-3 Δt dependence of the accuracy of the Monte Carlo simulation of the Na^+ ion under the electric field E. $< \Delta x^2 >_M$ and $< \Delta x^2 >_A$ are the mean square displacements in Δt . $< \Delta x^2 >_M$: Monte Carlo , $< \Delta x^2 >_A$: analytical result. T = 298K.

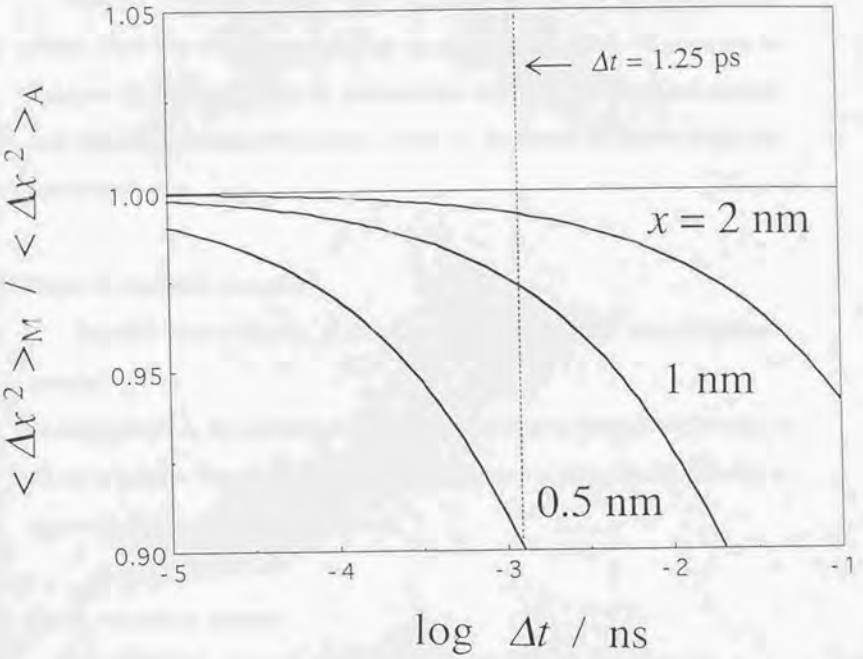

Fig.2-2-4 Δt dependence of the Accuracy of the Monte Carlo simulation of the Na^+ ion in the potential $U = -e^2 / 4\pi\varepsilon_0 \varepsilon x$. $< \Delta x^2 >_M$ and $< \Delta x^2 >_A$ are the mean square displacements in Δt . $< \Delta x^2 >_M$: Monte Carlo , $< \Delta x^2 >_A$: analytical result. $T = 298K$, $e = 1.60 \times 10^{-19}$ C, $\varepsilon_0 = 8.85 \times 10^{-12}$ F/m, $\varepsilon = 76.8$.

Error in Coulombic potential

Fig.2-2-5 shows the error of $< \Delta x^2 >$ for the aqueous Na^+ ion near a positive charge. Since two cations are not likely to approach each other, the error can be neglected. In the simulation of the polyelectrolyte solutions, two cations can approach each other on the surface of the polyion. However, the distance of them is longer than 2nm in many cases.

Error in harmonic potential

Fig.2-2-6 shows the error of $< \Delta x^2 >$ for the aqueous Na^+ ion in a harmonic potential.

As discussed in 2.4, the counterion in polyelectrolyte solution is harmonically bounded at the end of polyion. The potential of Fig.2-2-6 is the model of such potential. The error is expected to be below 1% for Δt = 1.25 ps.

Other simulation method

D.L.Ermak [9,10] proposed a simulation method based on the same Langevin equation discussed 1.1.

$$m\dot{x} = -\zeta \dot{x} + R(t) + F \tag{19}$$

In this method , the force F is assumed to be constant in a period of Δt.. Assuming the Smolchowski level approximation, eq(19) becomes:

$$0 = -\dot{x} + \frac{1}{\beta}\lambda(t) + \frac{1}{\beta} f \tag{20}$$

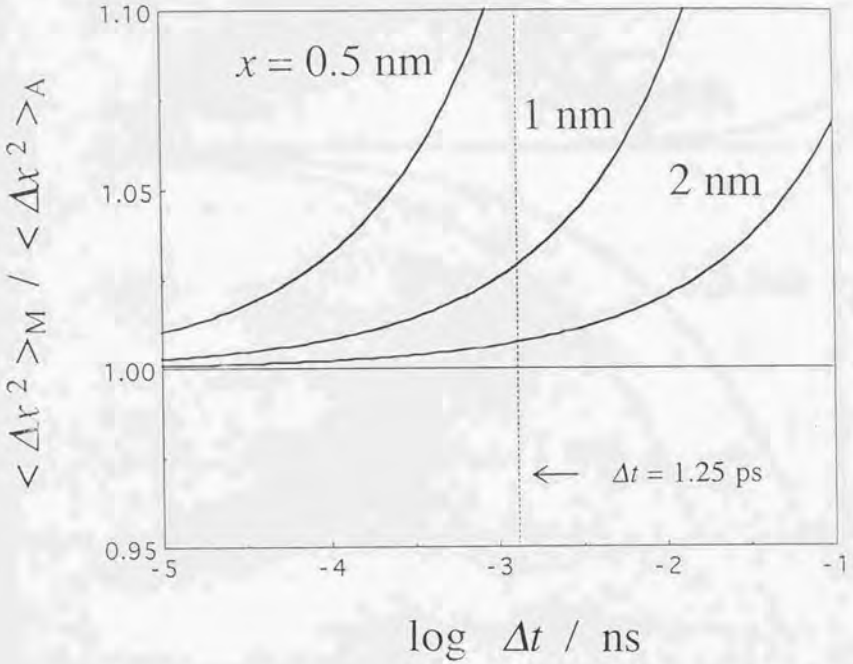

Fig.2-2-5 Δt dependence of the accuracy of the Monte Carlo simulation of the Na^+ ion in the potential $U = e^2 / 4\pi\varepsilon_0 \varepsilon x$. $< \Delta x^2 >_M$ and $< \Delta x^2 >_A$ are the mean square displacements in Δt . $< \Delta x^2 >_M$: Monte Carlo , $< \Delta x^2 >_A$: analytical result. $T = 298K$, $e = 1.60 \times 10^{-19}$ C, $\varepsilon_0 = 8.85 \times 10^{-12}$ F/m, $\varepsilon = 76.8$.

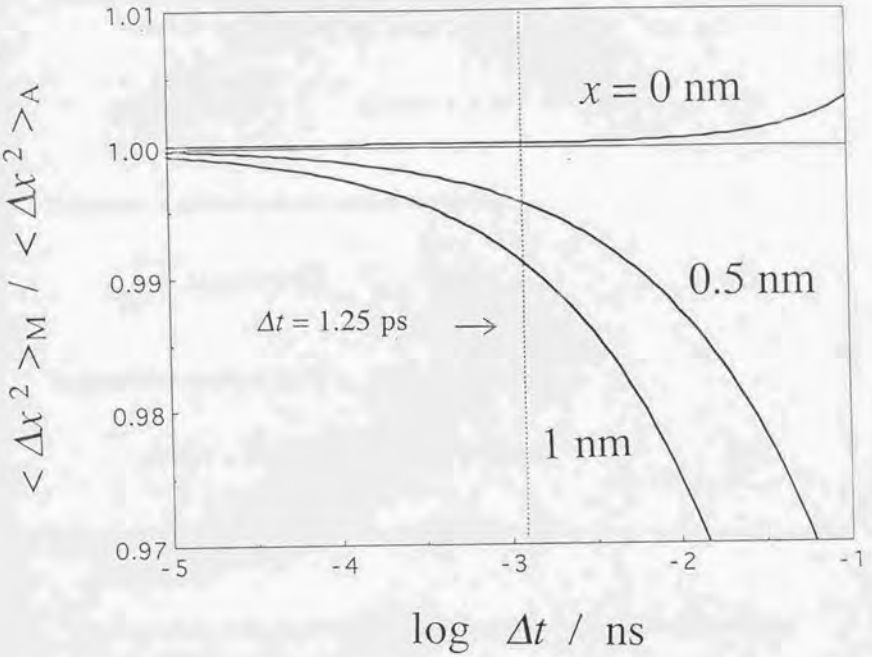

Fig.2-2-6 Δt dependence of the accuracy of the Monte Carlo simulation of the Na^+ ion in the potential $U = k\,x^2/2$. $< \Delta x^2 >_M$ and $< \Delta x^2 >_A$ are the mean square displacements in Δt. $< \Delta x^2 >_M$: Monte Carlo, $< \Delta x^2 >_A$: analytical result. T = 298K, $k = 1.0 \times 10^{-3}$ N/m.

where, $\beta = \zeta / m$, $\lambda(t) = R(t) / m$, $f = F / m$.

In this method, the time evolution of $x(t)$ is calculated by :

$$x(t+\Delta t) = x(t) + \int_t^{t+\Delta t} \lambda(\tau)\, d\tau + f\, \Delta t \tag{21}$$

The integral is assumed to be the random variable δx :

$$\int_t^{t+\Delta t} \lambda(\tau)\, d\tau = \delta x \tag{22}$$

The probability density of δx is :

$$p(\delta x) = (4\pi D\Delta t)^{-\frac{1}{2}} \exp(-\delta x^2 / 4D\Delta t) \tag{23}$$

If F in eq(19) is constant , eq(23) is analytically obtained.

The mean values of the displacement $< \Delta x >$ and $< \Delta x^2 >$ from this method agree with those of the Langevin equation in the order of Δt as well as the Monte Carlo method. $< \Delta x >$ and $< \Delta x^2 >$ up to the order of Δt^2 are written as:

$$< \Delta x > = - \frac{D}{k_B T} \left(\frac{\partial U}{\partial x} \right)_{x_0} \Delta t \tag{24}$$

$$< \Delta x^2 > = 2\, D\Delta t + \frac{D^2}{k_B^2 T^2} \left(\frac{\partial U}{\partial x} \right)_{x_0}^2 \Delta t^2 \tag{25}$$

The diversions of $< \Delta x >$ and $< \Delta x^2 >$ depend on the shape of the potential . In some cases, the diversion of this Ermak's method is smaller than that of the Monte Carlo method. However, the Brownian motion in a harmonic potential was successfully reproduced by both method.

2.2.4 Discussions

The Monte Carlo method has some advantages on the other methods for studying the dynamics in polyelectrolyte solutions.

The molecular dynamics (MD) is now a popular simulation technique and can provide the most precise information on the dynamics in the solutions. However, it requires much longer computation time than the MC method. The time step in MD simulation should be usually the order of 10^{-15} second, because the equation of motion should be stably solved for all the atoms in any situation. On the other hand, the time step in the MC simulation can be above 10^{-12} second, if the error of a few percents is allowed. Since no differential equation is solved in the MC algorithm, the computation continues without any trouble if the time step is too large for specific atoms incidentally. In addition , the computation time of the MD simulation becomes longer with the decrease of the solution concentration, because the motion of the solvent molecules should be considered as well as the solute molecules. The computation time of MC simulation does not depend on the concentration because the solvent is considered as continuum. There have been few reports on the MD simulation of electrolyte solutions.

The Langevin dynamics (LD) simulation is carried out by the numerical integration of the Langevin equation. Since the MC simulation in this work is also based on the Langevin equation, both simulations have the same physical meaning and should provide the same results. This method may be applicable to the polyelectrolyte solution, and the behavior of NaCl solution has been studied by this method, as discussed in section 3.2 . The LD method is almost equivalent to the MC method, however its algorithm is a little complicated in the case of considering discontinuous potentials, for example collisions of the ions.

Another possible approach for analyzing the behavior of the solute ions is the calculation of the diffusion equation. The diffusion equation is also based on the Langevin equation and the Smolchowski level approximation as well as the MC simulation. However, since the distribution

function is the multivariable function of the positions of all the ions, the algorithm becomes complicated and requires longer computation time. Some additional approximations such as the Debye-Huckel one have been introduced for solving the diffusion equation.

Therefore, the Monte Carlo simulation is suitable for studying the behavior of the solute ions in dilute aqueous solutions.

References

1) Metropolis, N., Rosenbush, A. W., Rosenbush, M. N, Teller, A. H., and Teller, E. *J. Chem. Phys.* **21** (1953) 1987

2) M.P.Allen and D.J.Tildesley, *Computer Simulation of Liquids (Clarendon press, oxford)*, 1987

3) Binder,K. ed., *Monte Carlo methods in statistical physics (Springer, Berlin)*, (1979)

4) Binder,K. ed., *Application of the Monte Carlo method in statistical physics, 2nd.Ed. (Springer, Berlin)*, (1987)

5) Kikuchi,K., Yoshida,M., Maekawa,T., and Watanabe,H. *Chem.Phys.Lett.* **185**, 335 (1991)

6) Kikuchi,K., Yoshida,M., Maekawa,T., and Watanabe,H. *Chem.Phys.Lett.* **196**, 57 (1992)

3. Applications

In this chapter , applications of the Monte Carlo simulation to polyelectrolyte solutions were shown and discussed. First of all, the Brownian motion in a harmonic potential was simulated in order to show the validity of the Monte Carlo simulation . Then, diffusion of ions in NaCl solution (section 3.2), rotational Brownian motion of a rod-like polyion (section 3.3), polarization of counterion atmosphere around a fixed polyion (section 3.3), and coupled rotational and ion atmosphere dynamics of a polyelectrolyte (section 3.4) were simulated and discussed.

3.1 Brownian motion in a harmonic potential

In order to demonstrate the applicability of the Monte Carlo method, the simulations of the Brownian particles in a harmonic potential were carried out. Then the time evolution of the distribution function and the mean square displacement were found to agree with the analytical results.

3.1.1 Analytical results from the Langevin equation.

We consider a Brownian particles in a harmonic potential:

$$U(x) = \frac{1}{2} k x^2 \tag{1}$$

The Langevin equation of the particle is:

$$m \ddot{x} = -k x - \zeta \dot{x} + \lambda(t) \tag{2}$$

As discussed in 2.1, we assume that the frictional force is so large that the left hand side of is considered to be zero. The analytical solution of the probability density $P(x,t)$ has been known as [1]:

$$P(x,t) = \left(\frac{k}{2\pi k_B T \{1 - exp(-(2k/\zeta)t)\}} \right)^{\frac{1}{2}} exp\left(-\frac{k}{2k_B T} \frac{x^2}{1 - exp(-(2k/\zeta)t)} \right) \quad (3)$$

and the mean square displacement is:

$$<(\Delta x)^2> = \frac{k_B T}{k} \{1 - exp(-(2k/\zeta)t)\} \quad (4)$$

3.1.2 Model and Simulation

The simulation was carried out by the Metropolis Monte Carlo method [2]. The auther considered the aqueous Na^+ ion in a harmonic potential. In polyelectrolyte solutions, the counterions are bounded harmonically near the polyion in some cases. The time step, Δt, is 1.0 ps, which was found to be short enough for this case, as is discussed in section 2.2. The results were obtained by accumulating 10,000 trajectories.

3.1.3. Results

Fig.3-1-1 shows the probability density of the particle at two different times. The results from the simulation well agree with the analytical results. Fig 3-1-2 shows the mean square displacement, $<(\Delta x)^2> = <(x(t) - x(0))^2>$, of the particles. These results were found to agree to the analytical ones.

3.1.4 Discussion

It was clearly demonstrated that the Monte Carlo simulation can be used for investigating the dynamic properties of the Brownian particles such as solute ions. The harmonic potential is one of the simplest examples of potentials. However, as discussed in chapter 2, more than second derivatives of potentials are mixed in the error of this simulation method.

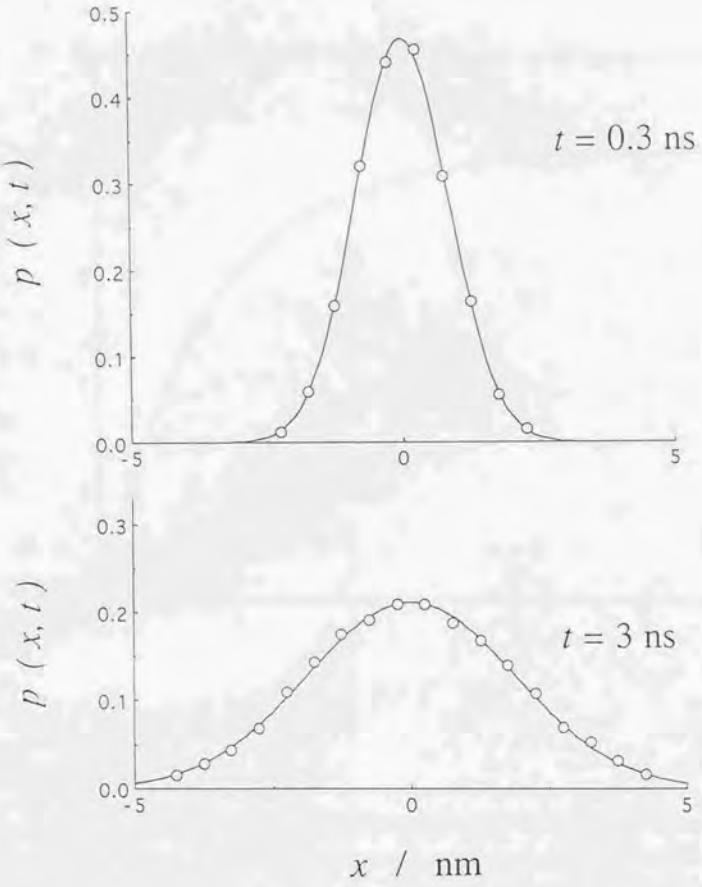

Fig.3-1-1 Probability density of the Brownian particle in the harmonic potential $U = kx^2 / 2$ ○: simulation (10,000 trajectories are accumulated) , solid line: theory. Initial condition: $x = 0$ at $t = 0$. $k = 1.0 \times 10^{-3}$ N/m , $T = 298$ K, $\zeta = 3.1 \times 10^{-12}$ kg/s , $\Delta t = 1$ ps.

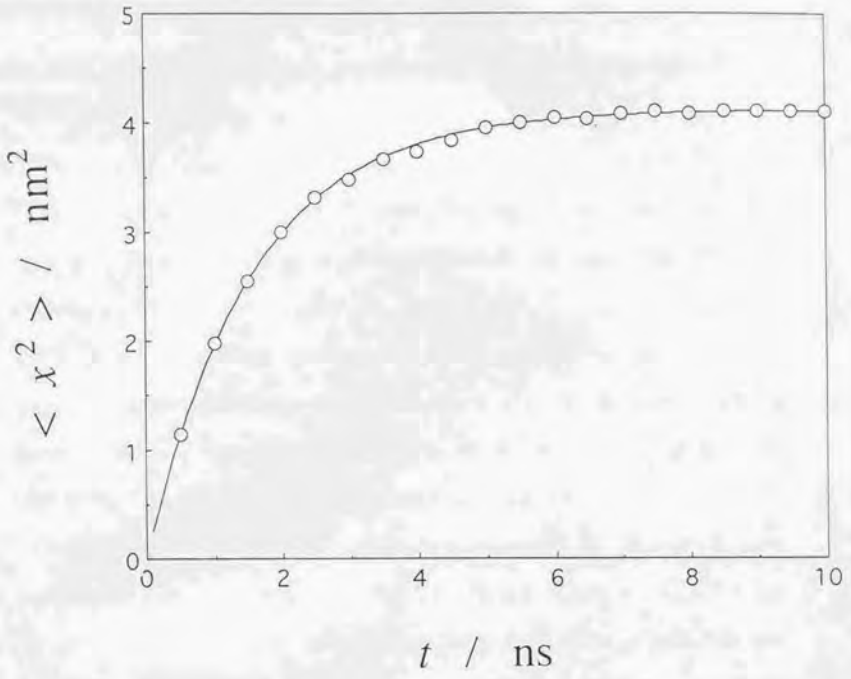

Fig.3-1-2 Time evolution of $< x^2 >$ of the Brownian particle in the harmonic potential $U = kx^2 / 2$ ○: simulation (10,000 trajectories are accumulated) , solid line: theory. Initial condition: $x = 0$ at $t = 0$. $k = 1.0 \times 10^{-3}$ N/m, $T = 298$ K, $\zeta = 3.1 \times 10^{-12}$ kg/s , $\Delta t = 1$ ps.

References

1) Uhlenbeck,G.E. and Ornstein,L.S. *Phys.Rev.*, **36**, 823(1930)

2) Kikuchi,K., Yoshida,M., Maekawa,T., and Watanabe,H. *Chem.Phys.Lett.* **185**, 335(1991)

3. 2 Diffusion of ions in NaCl solution

It is very important to investigate the motion of the aqueous Na^+ and Cl^- ions , because the Na^+ ion is the most common counterion in polyelectrolyte solutions, and NaCl are a popular added salt in the experiments.

There have been some computational studies on the NaCl solutions. Wood and Friedman [1] calculated the diffusion coefficient by solving the Smolchowski equation (diffusion equation) . Turq et al[2] obtained the diffusion coefficient by solving the generalized Langevin equation.

The Mante Carlo simulation has been used for calculating the ion distribution and the thermodynamic quantities. Card et al.[3] obtained the excess energy, the heat capacity, and the osmotic pressure. Sφrensen et al. [4] carried out more precise simulations of dilute NaCl solution. Their results agreed with those from the Debye Huckel theory.

The diffusion coefficients of ions in electrolyte solutions have been measured by using the isotopes. Mills [5] measured the diffusion coefficients of ions in several 1:1 salt solutions. Especially, the concentration dependence of the diffusion coefficient was precisely obtained for NaCl solutions. The concentration dependence from our results was found to agree to that by Mills.

3.2.1 Model

The model system is shown in Fig.3-2-1. The restrictive primitive model [3] was used for Na^+ ions and Cl^- ions. In this model, all the ions are considered to be hard spheres with point charges. The minimum distance R_{min} between Na^+ and Cl^- ions was chosen to be

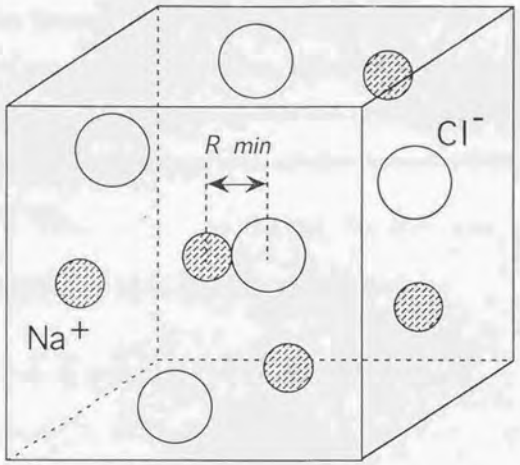

Fig.3-2-1 Model of the NaCl solutions.

0.425 nm . Card carried out the simulations using this restrictive primitive model, and calculated several thermodynamic quantities such as excess internal energy, heat capacity , and osmotic pressure. These calculated values have been reported to agree with the experimental data for R_{min} = 0.425 nm. Thus, this value has not been proved to be appropriate for calculating dynamic quantities such as the diffusion coefficients. However, as shown below, the diffusion coefficients calculated from our simulations also agree to the experimental data.

The potential energy for the Metropolis scheme is given as:

$$U = \sum_i \sum_j \frac{z_i z_j e^2}{4 \pi \varepsilon_0 D r_{i,j}} + \sum_i \sum_j U_1(r_{ij}) \qquad (1)$$

where r_{ij} is the distance between i th ion and j th ion, z_i is valence of i-th ion, D is the dielectric constant of water at 25 C. The second term is a short range interaction such as the effect of the exclude volume. Since the restrictive primitive model is used, $U_1(r_{ij})$ becomes:

$$U_1(r_{ij}) = \begin{cases} \infty & r_{ij} < R_{min} \\ 0 & r_{ij} \geq R_{min} \end{cases} \qquad (2)$$

3.2.2 Simulation

The simulations were carried out by the Metropolis scheme. The periodic boundary condition was imposed. The 26 image cells and all the interactions between the ions in the unit cell and the image cells. The maximum displacement d_{max} for Na ions and Cl ions are calculated from:

$$d_{max}^2(Na^+) = 6\, D_0(Na^+)\, \Delta t \tag{3}$$

$$d_{max}^2(Cl^-) = 6\, D_0(Cl^-)\, \Delta t \tag{4}$$

where, $D_0(Na^+)$ (= 1.33 m^2/s) and $D_0(Cl^-)$ (= 2.00 m^2/s) are the diffusion coefficients of Na^+ ions and Cl^- ions in the infinite dilute solution. The time step Δt is chosen to be 1.25 ps . The number of the Na^+ ions N in the unit cell is 30 in many cases. We carried out several simulations for N = 30, 60, and 100. The diffusion coefficients obtained from them were found to be equal within 5%.

3.2.3 Results

The positions of Na ions and Cl ions are recorded every 10 steps. Several kind of motions were observed. In the short time range, the ions shows the rotational and vibrational motions. In the long time range, the ions shows diffusion processes, which satisfies the Einstein law. We discuss about the motion of the ions in terms of the following quantity:

$$D(\tau) = \frac{< (x(t+\tau) - x(t))^2 >}{6\tau} \tag{5}$$

where, the < > represents the average over all the ions .

Fig.3-2-2 shows $D(\tau)$ of the both ions. These values decrease with the increase of the sampling time τ. The broken lines in this figure shows the diffusion coefficients in infinite dilute solutions. The large $D(\tau)$ for small τ result from their rotational and vibrational motion in short time range. The diffusion speed $D(\tau)$ converges for large τ . Such a

dependence of $D(\tau)$ on τ results from the Coulombic interactions between the ions. Fig.3-2-3 shows $D(\tau)$ obtained the simulations in which the Coulombic interactions are ignored. In this case, $D(\tau)$ is independent of the time interval τ.

Since $D(\tau)$ converges for large τ, the diffusion coefficient can be calculated by:

$$D = \lim_{\tau \to \infty} \frac{< (x(t+\tau) - x(t))^2 >}{6\tau} \qquad (6)$$

This is the definition of the diffusion coefficients usually used in experiments. Therefore, the calculated values according to the definition above can be compared to the experimental data.

The diffusion coefficients of the ions obtained from our simulation well agree to the experimental results. Fig.3-2-4 shows the concentration dependence of the diffusion coefficients of Na ions. Fig.3-2-5 shows that of Cl ions. In these simulations, the system consist of 30 Na ions and 30 Cl ions. The diffusion coefficients were calculated from the mean square displacement during over 12.5 ns.

In these simulations, the diameter of the both ions R_{min} was set to be 0.425 nm as discussed above. In order to investigate the effect of the diameter, several simulations were carried out for R_{min} = 0.5 nm and R_{min} = 0.6 nm. The diffusion coefficients obtained from the both simulations were found to be lower than those for R_{min} = 0.425 nm

The diffusion coefficient depends on the solvent. Several simulations were carried out for different dielectric constant. The diffusion coefficient was found to decrease with the decrease of their dielectric constant. The decrease of the dielectric constant causes strong interaction between the ions. In our simulation scheme, the decrease of the dielectric constant of the solvent is completely same as the decrease of the temperature. Therefore, the decrease of the diffusion coefficient can be the influence of the low temperature. However,

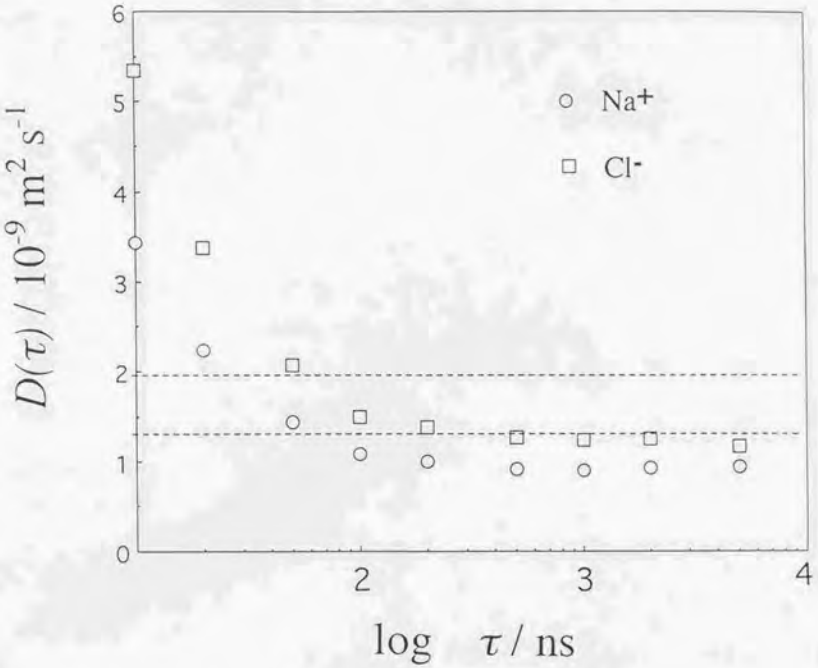

Fig.3-2-2 Dependence of $D(\tau)$ ($=\langle x(t+\tau)-x(t)\rangle/6\tau$) on the duration τ in the 1M NaCl solution.

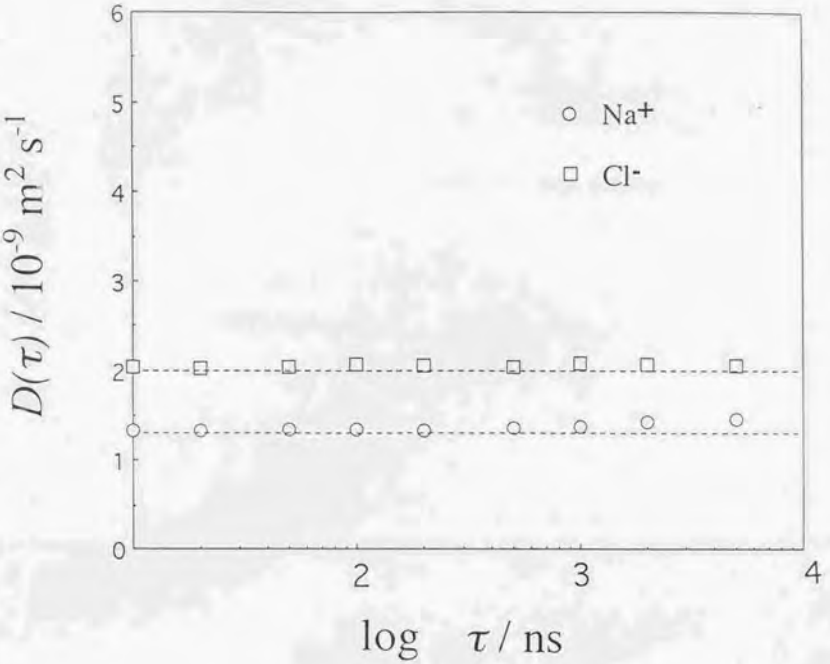

Fig.3-2-3 Dependence of $D(\tau)$ $(=\langle x(t+\tau)-x(t)\rangle/6\tau)$ on the duration τ in a hypothetical 1M NaCl solution (Coulombic interactions are neglected).

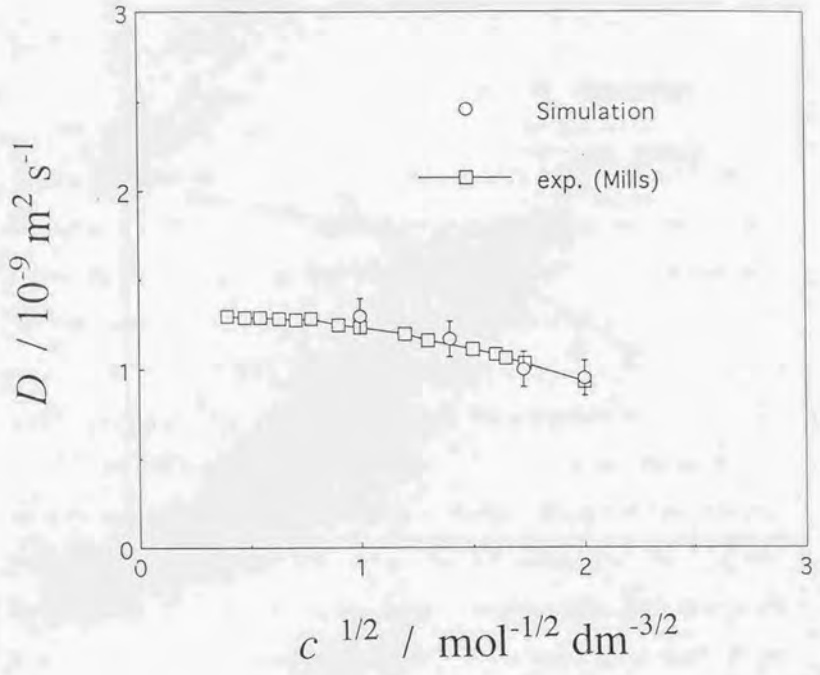

Fig.3-2-4 Concentration dependence of the diffusion coefficient of Na ions.

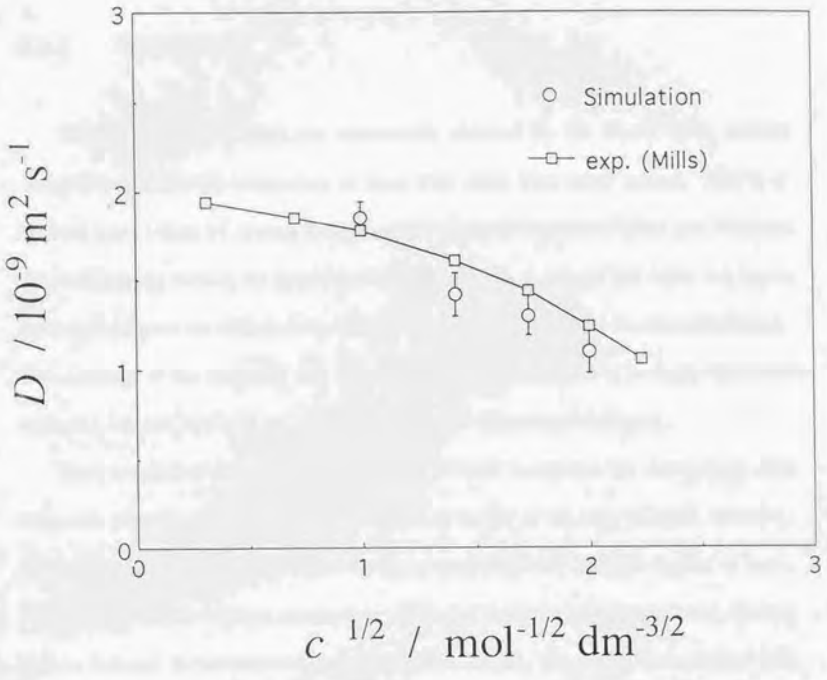

Fig.3-2-5 Concentration dependence of the diffusion coefficient of Cl ions.

the diffusion coefficient is not proportional to the square root of the temperature. This means that the motion of the ions are not only thermal ones.

3.2.4 Discussion

The diffusion coefficients are successfully obtained by the Monte Carlo method. Table 3-2-1 shows the comparison of them with those from other method. Turq et al. obtained these values by solving the generalized Langevin equation. Wood and Friedman obtained them by solving the Smolchowski equation. As is seen in this table, our Monte Carlo method gives the diffusion coefficients with a equal accuracy to other calculations. The advantage of our method is that the time step Δt can be chosen to be larger than these methods (Monte Carlo 1.25 ps, other two methods : the order of 0.01 ps) .

There are several subjects to be considered in order to improve our simulations. The restrictive primitive model causes the satisfactory results in the case of NaCl solutions. However, this model can not be used for the system with more than two species of ions . Furthermore, the hard sphere assumption can not be made for more complicated systems such as colloidal suspensions and polyelectrolyte solutions. Therefore, the models of inter molecular potentials for these systems are desired to be developed.

The boundary conditions should be considered more precisely. The use of Ewald method is preferable for systems with long range interactions such as the Coulombic potentials. We have already developed the program including the Ewald method. Several simulations with the Ewald method were carried out. However, no significant differences were observed between the simulations with and without the Ewald method. Card et al. successfully obtained the thermodynamic quantities in NaCl solutions without using the Ewald method. Therefore, the Ewald method was not applied to the simulations in this

Table 3-2-1 Diffusion coefficients of the Na^+ and Cl^- ions in the 1M NaCl solution.

	D / 10^{-9} m^2 s^{-1}		Δt / ns	
	Na^+	Cl^-		
Monte Carlo Simulation	1.25	1.92	1.25	
Turq et.al.	1.30	1.90	0.012 (Na)	0.029(Cl)
Wood et.al.	1.272	1.859	0.005	
Mills (experiment)	1.234	1.77	-	

work in order to reduce the computational time.

The hydrodynamics interactions should be taken into account in order to improve our simulations. We have already developed the program with the hydrodynamic interactions [6]. The simulation with the hydrodynamic interactions requires much long calculation time , because thousands of correlated random numbers should be generated. However, the hydrodynamics interactions play significant roles in the systems including various size of particles.

References

1) Wood, D. M. and Friedman, H. L. *Zeitschrift fur Physikalische Chemie Neue Folge*, bd. 155, S.121-132 (1987)

2) Turq, P and Lantelme, F *J.Chem.Phys.* , **66**, 3039 (1977)

3) Card,D.N. and Valleau,J.P. J. Chem. Phys., **52**, 6232 (1970)

4)Sφrensen,S., Sloth,P., and Nielsen,H.B., and Birger,J. *Chemica Scandinavica* A42, 237 (1988)

5) Mills,R *Reviews of Pure and Applied Chemistry*

6) Kikuchi,K., Yoshida,M., Maekawa,T., and Watanabe,H. *Chem. Phys. Lett.*, **196**, 57 (1992)

3.3 Rotational Brownian motion of rod-like polyion

Polyelectrolyte solution containes large polyions and small counterions . The motion of the counterion such as Na^+ can be simulated by the Monte Carlo method as discussed in 3.2. However the rotational motion of the polyion is important phenomenon in polyelectrolyte solutions, beause orientational motion of polyions is detected in the electro-optical measurements. Therefore the rotational Brownian motion was discussed in this section. The Monte Carlo simulation is applicable to the rotational Brownian motions as well as the translational ones. However, the scheme can not be directly applied to the polar coordinate systems, because the absolute value of the trial displacement should be independent of the position. The algorithm for this spherical diffusion was shown in section 3.3.2

3.3.1 Model

A rod like molecules with a permanent or induced dipole moment was considered (Fig.3.3.1). Its center was fixed and it shows anisotropic distributions under the external electric field. In this work, the orientational motion of this molecule was simulated by the Monte Carlo method. This corresponds to the assumption that the rotational relaxation time is much shorter than that of translational one.

The orientation of the molecules is usually expressed by the following orientation function:

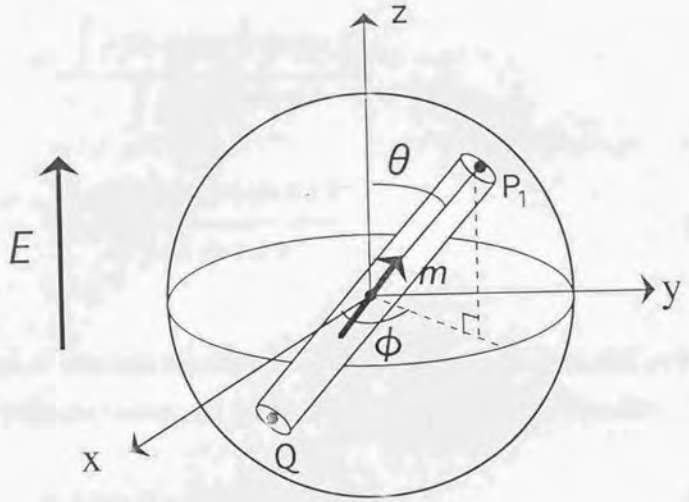

Fig.3-3-1 Model of the rod-like polyion with the dipole m.

$$\Phi = < P_2 (\cos \theta) >$$

$$= \frac{\int \rho(\theta) P_2 (\cos \theta) \sin \theta \, d\theta}{\int \rho(\theta) \sin \theta \, d\theta}$$

$$= \frac{\int \rho(\theta) P_2 (\cos \theta) \sin \theta \, d\theta}{\int \rho(\theta) \sin \theta \, d\theta} \qquad (1)$$

where, θ is the angle between the axis of the rod and the direction of the field, $\rho(\theta)$ is the distribution function , and $P_2(x)$ is the second order Legendre polynomial :

$$P_2 = (\cos \theta) = \frac{3 \cos^2 \theta - 1}{2} \qquad (2)$$

The electric birefringence signal [2] is proportional to this value, if the optical polarizability has cylindrical symmetry. The steady state value of Φ is calculated from the Botzmann distribution for $\rho(\theta)$:

$$\rho(\theta) = \rho \, exp\left(-\frac{U(\theta)}{k_B T}\right) \qquad (3)$$

where, $U(\theta)$ is the potential energy and ρ is a normalization constant. The dipole moment m under the electric field E is written as:

$$m = \mu + \alpha E + o(E) \qquad (4)$$

where, μ is the permanent dipole moment and α is the electric polarizability. The potential

energy of the rod under the electric field is given by :

$$U(\theta) = -\mu E \cos(\theta) - \frac{1}{2} \alpha E^2 \cos^2(\theta) + o(E^2) \tag{5}$$

The time evolution of the distribution function $\rho(\theta, t)$ is assumed to be given by the following diffusion equation:

$$\frac{\partial \rho}{\partial t} = D \nabla^2 \rho - D \, div \left(\rho \frac{M}{k_B T} \right) \tag{6}$$

where, D is a rotational diffusion coefficient, and M is the torque which effect the molecule. The relaxation of the orientation function without the external field is obtained from the diffusion equation above :

$$\Phi = \Phi_0 e^{-6Dt} \tag{7}$$

where, Φ_0 is the initial value of the orientation function. The time evolution of Φ under week fields can be written simply for the following two cases. If the molecule has only a permanent dipole moment μ, the time evolution of Φ has been known as [1] :

$$\Phi = \Phi_0 \left(1 - \frac{3}{2} e^{-2Dt} + \frac{1}{2} e^{-6Dt} \right) \tag{8}$$

where, Φ_0 is the initial value of Φ, and D is the rotational diffusion coefficient in the diffusion equation above. And if the molecule has a induced dipole moment which is parallel to its axis, it has been known as:

$$\Phi = \Phi_0 (1 - e^{-6Dt}) \tag{9}$$

In this thesis, two simulations corresponding to eq(8) and eq(9) were carried out .

3.3.2 Metropolis scheme for rotational motion

Fig.3-3-2 shows the main part of the scheme. The maximum rotation d_{max} should be chosen:

$$d_{max}{}^2 = 6\,D\,\Delta t \qquad (10)$$

where, D is the rotational diffusion coefficient. The characteristic of this algorithm is that the displacement on the sphere is expressed by the rotation along the longitude and that along the large circle. Therefore ϕ' in Fig.3-3-2 is complicated.

The displacement on a sphere $(P_1 \rightarrow P_2)$ is expressed by two angle $\Delta\theta$ and $\Delta\psi$. The angle $\Delta\theta$ corresponds to the rotation along the longitude. The angle $\Delta\psi$ corresponds to the rotation along the large circle, which makes a right angle with the longitude at P_1. The direction of Ψ is same as that of the bearings ϕ. We consider that a point at $P_1\,(\theta_1, \phi_1)$ moves to $P_2\,(\theta_2, \phi_2)$ by the rotations $\Delta\theta$ and $\Delta\phi$. The new position $P_2\,(\theta_2, \phi_2)$ is obtained by the following procedure.

(1) The rotation $\Delta\theta$ does not change ϕ, therefore θ_2 and ϕ_2 are:

$$\theta_2 = \theta_1 + \Delta\theta \qquad (11)$$

$$\phi_2 = \phi_1 \qquad (12)$$

(2) The rotation $\Delta\psi$ along the large circle mentioned above change both θ and ϕ. For simplicity, the bearings ϕ is assumed to be zero, then the large circle and the ψ axis are in

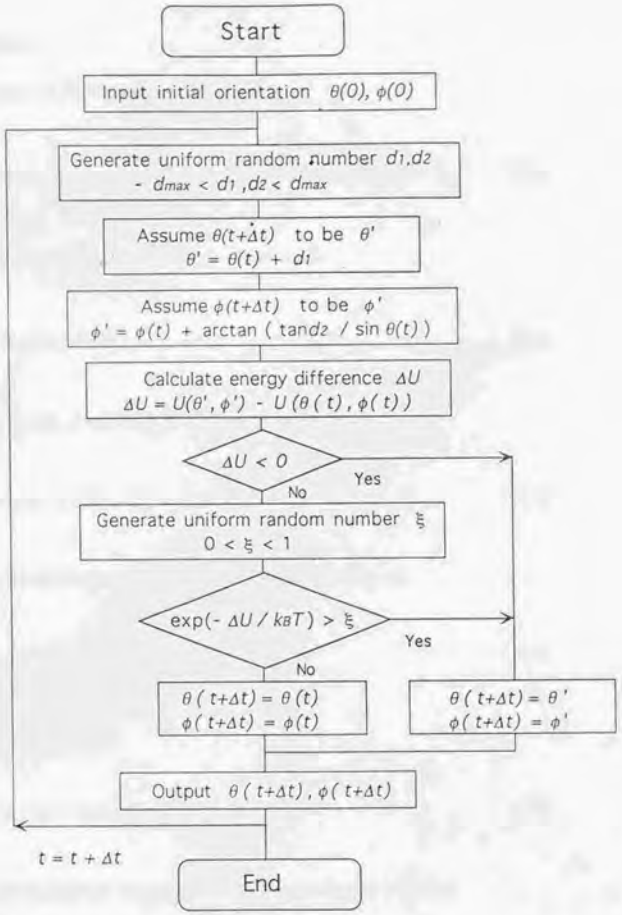

Fig.3-3-2 Metropolis Monte Carlo schme for the rotational Brownian motion.

the same plane.

(i) The height of P_2 from the z=0 plane is:

$$h = \cos(\Delta\psi)\sin(\pi/2 - \theta_1) = \cos(\Delta\psi)\cos\theta_1 \qquad (13)$$

because the the projection of OP_2 to y = 0 plane is:

$$l_1 = \cos(\Delta\psi) \qquad (14)$$

On the other hand, h can also be written by using θ_2 :

$$h = \sin(\pi/2 - \theta_2) = \cos\theta_2 \qquad (15)$$

Comparing these two expressions for h , θ_2 is obtained as :

$$\cos\theta_2 = \cos(\Delta\psi)\cos\theta_1 \qquad (16)$$

therefore,

$$\theta_2 = \cos^{-1}(\cos(\Delta\psi)\cos\theta_1) \qquad (17)$$

(ii) The x component of the projection of OP_2 to the x-y plane is:

$$l_2 = l_1\cos(\pi/2 - \theta_1) = \cos(\Delta\psi)\sin\theta_1 \qquad (18)$$

and ψ component is:

$$l_3 = \sin(\Delta\psi) \qquad (19)$$

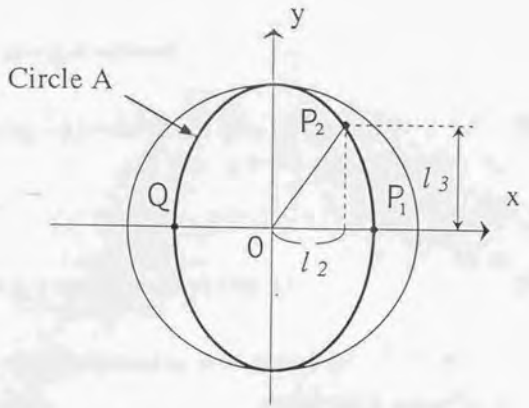

Fig.3-3-3 Projection on the z=0 plane.

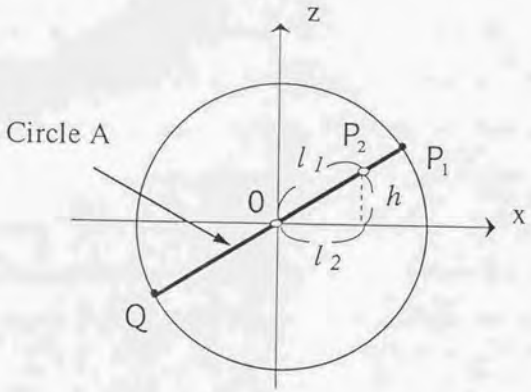

Fig.3-3-4 Projection on the y=0 plane.

Therefore , $\phi_2 - \phi_1$ is written as:

$$\tan(\phi_2 - \phi_1) = \sin(\Delta\psi) / \{\cos(\Delta\psi) \sin\theta_1\} \quad (20)$$

then

$$\phi_2 = \phi_1 + \tan^{-1}(\tan(\Delta\psi) / \sin\theta_1) \quad (21)$$

Thus , θ_2 ϕ_2 are expressed by $\Delta\theta$ and $\Delta\psi$.

3.3.3 Results

Fig.3-3-5 shows the relaxation process of the polyions. The polyion was parallel to the z axis at $t = 0$, then the initial value of Φ was unity. The time evolution of Φ is obtained from eq (7) and it was found to agree with the theoretical curve. Therefore, it was proved that the Monte Carlo simulation can be used for the rotational Brownian motion.

Fig 3-3-6 shows the orientation process of the polyion under the external electric field. The direction of the polyion was random at $t = 0$, then the initial value of Φ was zero. The theoretical curves were obtained from eq (8) for the induced dipole moment and eq(9) for the permanent dipole moment. The rise of Φ was found to be slightly faster than the theoretical curve, because eq(8) and eq(9) are obtained for infinitely weak field.

3.3.4 Discussion

As discussed above, the simulations of the polyion with the dipole moment were carried out in order to check the algorithm. In addition, these simulation can be used for analysis of the electro-optical measurements. Fig.3-3-7 shows the simulated responses of the electric birefringence measurements. In this thesis, only two type of dipole moments were considered, however simulations can be carried out for any kind of dipole moment which is described as a function of the angle θ and the field strength E. Thus, the Monte Carlo simulation is also a helpful tool for theoretical approach of the electro-optical measurements.

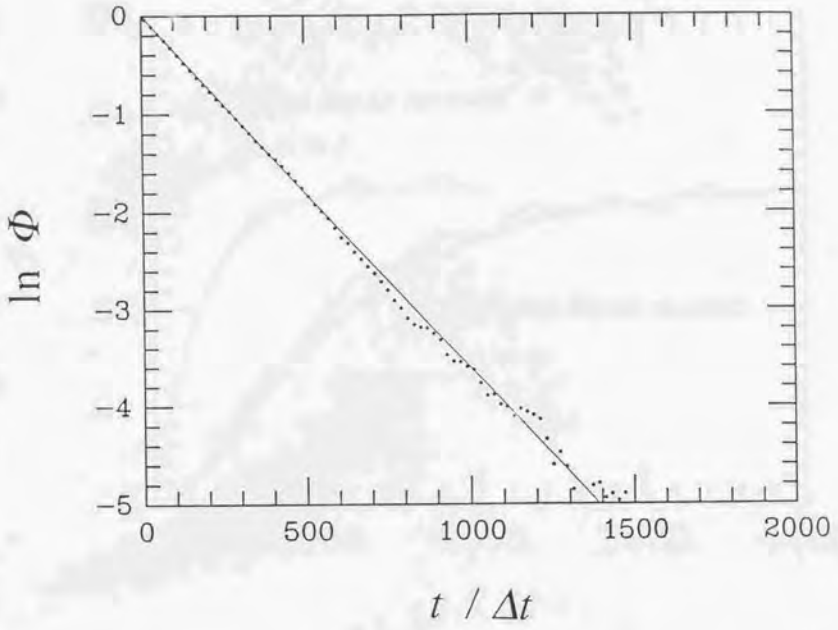

Fig.3-3-5 Decay process of the orientation factor $\Phi(t) = < p_2(\cos\theta(t))>$. The polyion is parallel to the z axis at $t = 0$. ●: simulation (100,000 trajectories are accumulatied) , solid line: theory.

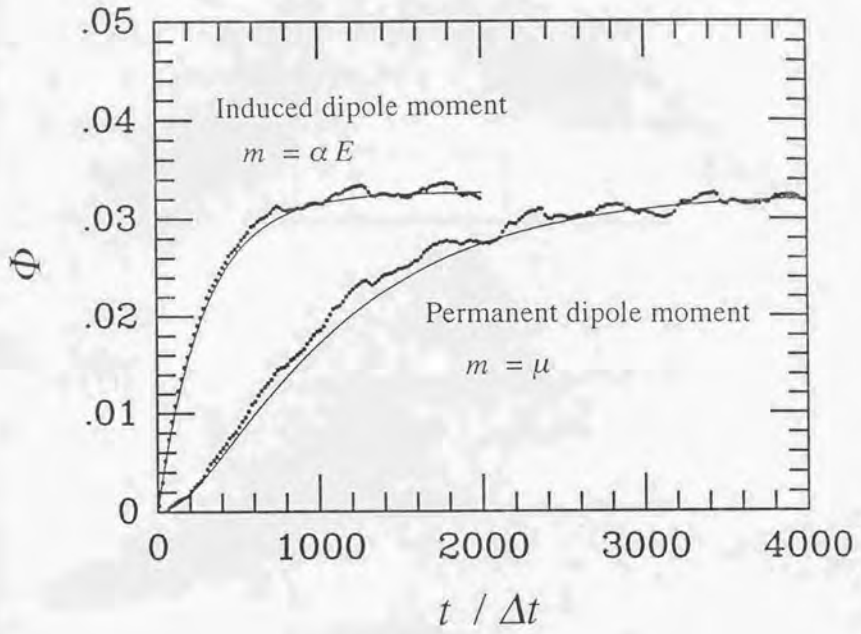

Fig.3-3-6 Rise process of the orientation factor $\Phi(t) = < p_2(\cos\theta(t))>$. The polyion is randomly oriented at $t = 0$, the external electric field is applied parallel to the z axis ($t > 0$). ●: simulation (500,000 trajectories are accumulatied) , solid line: theory. $\mu E / k_B T = 0.7$, $\alpha E^2 / k_B T = 0.7$.

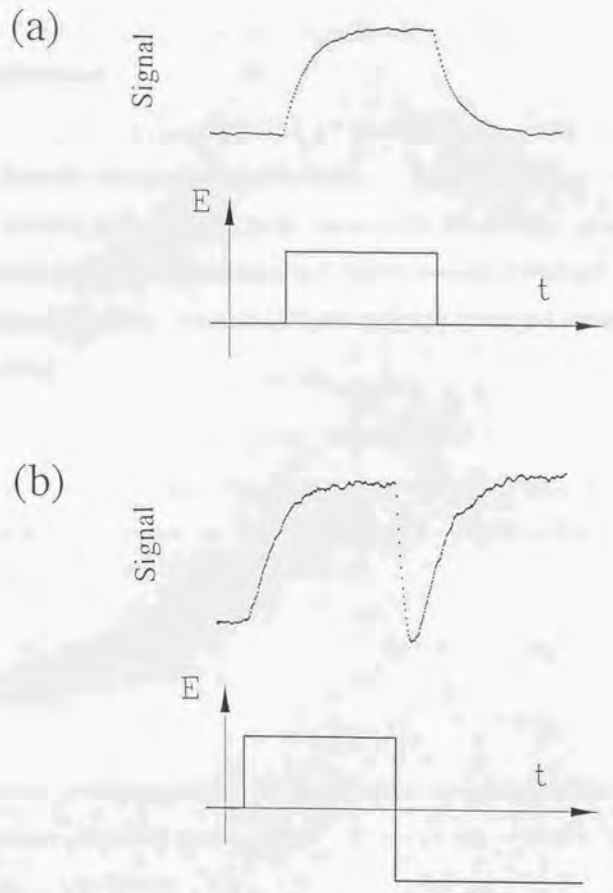

Fig.3-3-7 Simulation of the electrobirefringence measurement. (a) DC pulse measurement of the molecules with the induced dipole moment. (b) Reversing pulse measurement of the molecules with the permanent dipole moment.

References

1) Benoit,H *Ann. de phys.* , **6**, 561 (1951)

2) O'conski, C. T., and Zimm, B. H. *Science*, **111**, 113 (1950)

3) Kikuchi,K., Yoshida,M., Maekawa,T., and Watanabe,H.,*Colloid and Molecular Electro-Optics 1991 (Institute of Physics Publishing Bristol and Philadelphia)* , 7 (1991)

3.4 Polarization of polyelectrolyte solution

The motion of the counterions in polyelectrolyte solutions were investigated by the Monte Carlo simulation. In this section, the author focused on the effect of external electric fields. That is, the origin of the induce dipole moment of polyelectrolyte was discussed. Furthermore, the relaxation times of the polarization were successfully obtained.

3.4.1 Model and Simulation

The models used in this work are shown in Fig.3-4-1. The model of the polyion is a cylinder, which is fixed at the center of the unit. It has negative point charges on its axis at intervals of the separation , b. The effect of the charge density has been discussed in terms of ξ parameter:

$$\xi = e^2 / 4 \pi \varepsilon_0 b D k_B T \qquad (1)$$

where, e is the quantum of electricity, ε_0 is the permittivity of vacuum, and D is the dielectric constant of water at temperature T. Then separation b is written as $b = \xi l_B$, where l_B is the Bjerrum length:

$$\ell_B = \frac{e^2}{4 \pi \varepsilon_0 D k_B T} \qquad (2)$$

The model of the counter ion is a hard sphere with a positive point charge at its center. The number of counter ions is determined so that the net charge in the system is zero. The

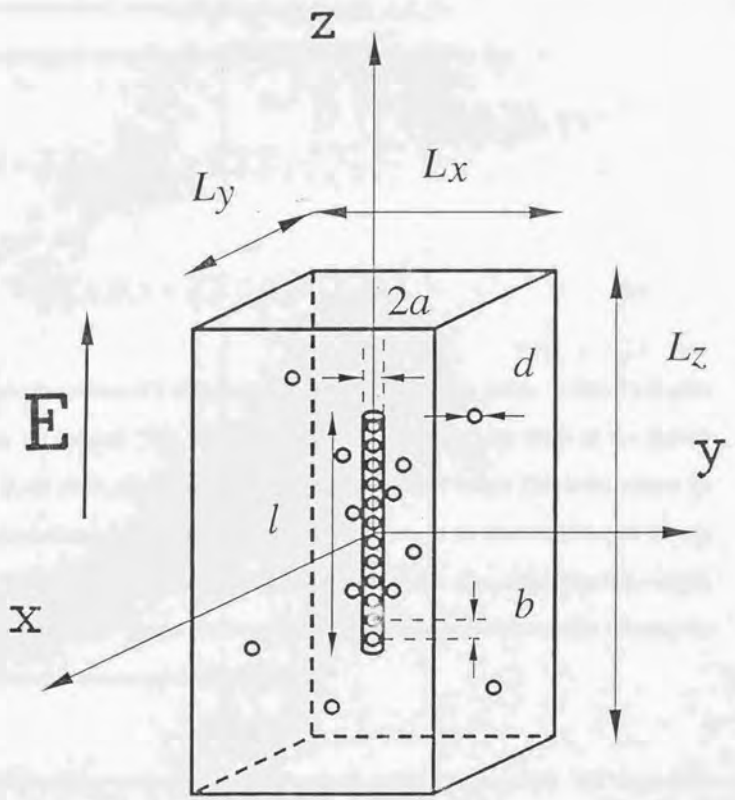

Fig.3-4-1 Model of polyelectrolyte solutions

concentration of the solution were expressed by two unit: polyion concentration C_P and residue concentration (counterion concentration) $C_R = N C_P$.

The energy of the system for the Metropolis scheme is given by:

$$U = \sum_i \sum_j \frac{z_i z_j e^2}{4 \pi \varepsilon_0 D r_{ij}} + \sum_i \sum_k \frac{z_i z_k e^2}{4 \pi \varepsilon_0 D r_{ik}}$$

$$+ \sum_i \sum_j U_1(r_{ij}) + \sum_i \sum_k U_1(r_{ik}) + \sum_i e \vec{E} \vec{r}_i \qquad (3)$$

where, z_i is the valence of i th counter ion, z_j is that of j th one, and z_k is that of k th point charge on the polyion. The third and fourth terms represent the effect of the exclude volume. In this work, it is considered as the repulsion of hard bodies. This is the same as the restrictive primitive model discussed in section 3.2 . Since all the movable ions have positive charges in this work, they are not likely to approach each other. Therefore, the exclude volume of the counter ions is not important. The last term is the interaction between the counter ions and the external electric field.

Simulations were carried out by the Metropolis Monte Carlo method. The unit cell for the simulation consists of one polyion and some counter ions. Periodic boundary condition is imposed. The unit cell are surrounded by 26 image cells. In many cases , the image cells have little influence on the results of the simulation because the counter ions are distributed near the polyions. Since the simulations of dynamic processes requires long time, the simulations were carried out using two image cells (Fig.3-4-2).

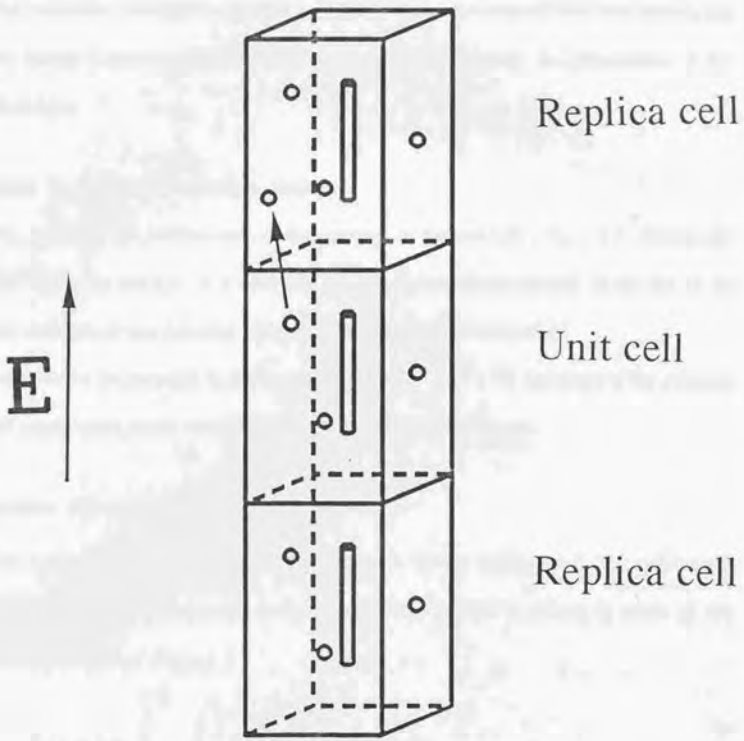

Fig.3-4-2 Replica cells in the case of calculating the relaxation times.

3.4.2 Results(1) Counterion distribution without field

The counterion distribution around a polyion without the external field was investigated by the Monte Carlo simulation. This is a basis of considering the polarization of the polyelectrolyte.

Potential in the polyelectrolyte solution

Fig. 3-4-3 is the contour map of the potential in the unit cell. Fig.3-4-4 shows the potential along the surface. It is seen that the potential increases sharply at the end of the polyion, such a well-like potential corresponds to conventional theories.

Fig.3-4-5 shows the potential in the function of $r = (x^2 + y^2)^{1/2}$, the shape of the potential curve is almost same as the coulomb potential by the negative charge.

Counterion distribution

The amount of counter ions near the polyion is shown in Fig.3-4-6. The polyions is represented by a hatched rectangle at the bottom. The amount is shown in terms of the number of counter ions $P(z,r_0)$:

$$P(z, r_0) = \int_{z-\frac{b}{2}}^{z+\frac{b}{2}} \int_{0}^{r_0} \rho(z, r)\, 2\pi r\, dr\, dz \qquad (4)$$

That is, $P(z,r_0)$ is the number of counterions in a cylinder of radius r_0 and height b. The number of ions was found to be almost independent of the position along the polyion, except at the end of the polyion. This sharp decrease has been known as the end effect. Fig.3-4-7 shows the polyion length dependence of the end effect. The decrease of the number of the counterions becomes sharper with the increase of the polyion length.

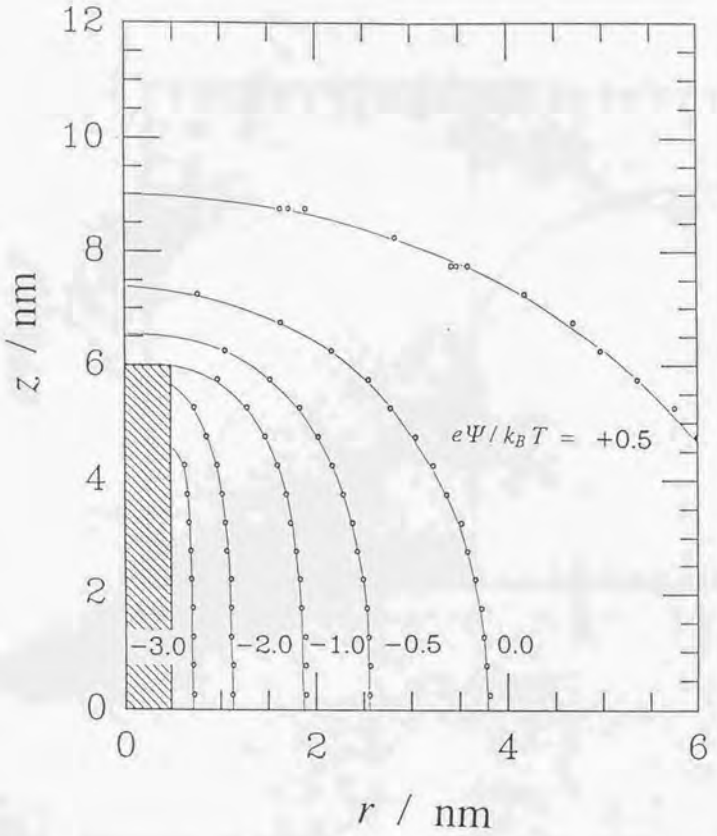

Fig.3-4-3 Contour map of the potential Ψ . ξ =1, T = 298 K, l = 12nm, N = 16, concentration of polyion: c_P = 3.0mM, concentration of counterion : c_R = 48mM.

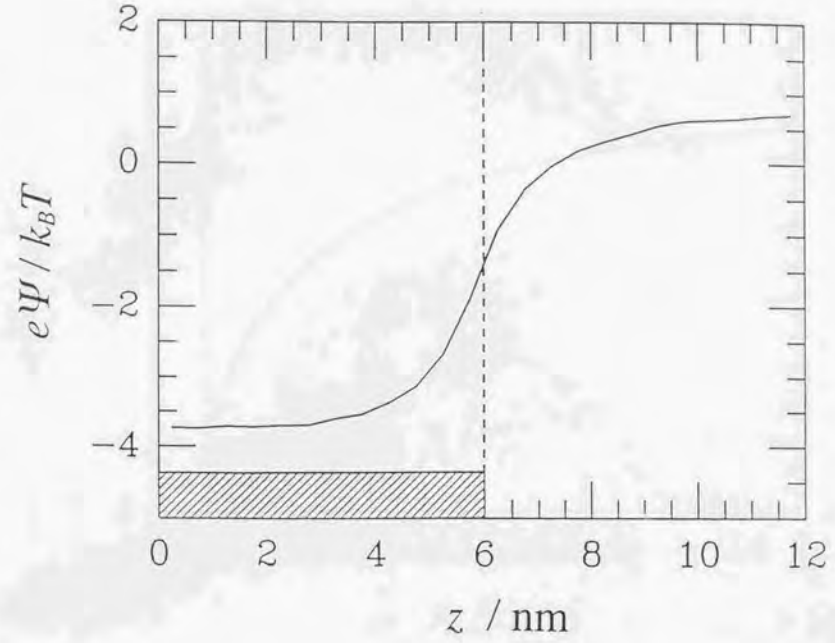

Fig.3-4-4 Potential Ψ along the polyion surface ($r = 0.5$). ξ=1, T = 298 K, l = 12nm, N = 16, c_P = 3.0mM c_R = 48mM.

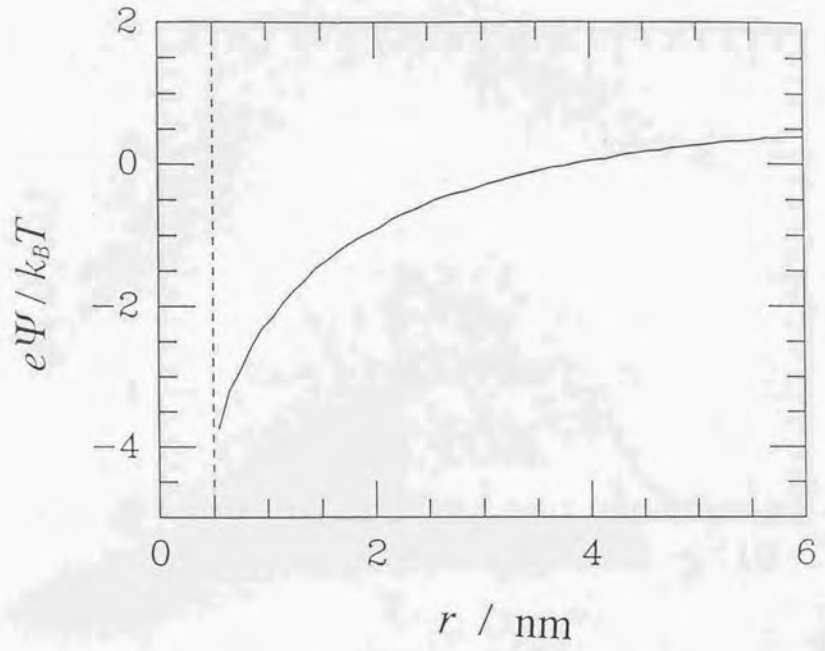

Fig.3-4-5 Potential Ψ in z = 0 plane. ξ =1, T = 298 K, l = 12nm, N = 16, c_P = 3.0mM c_R = 48mM.

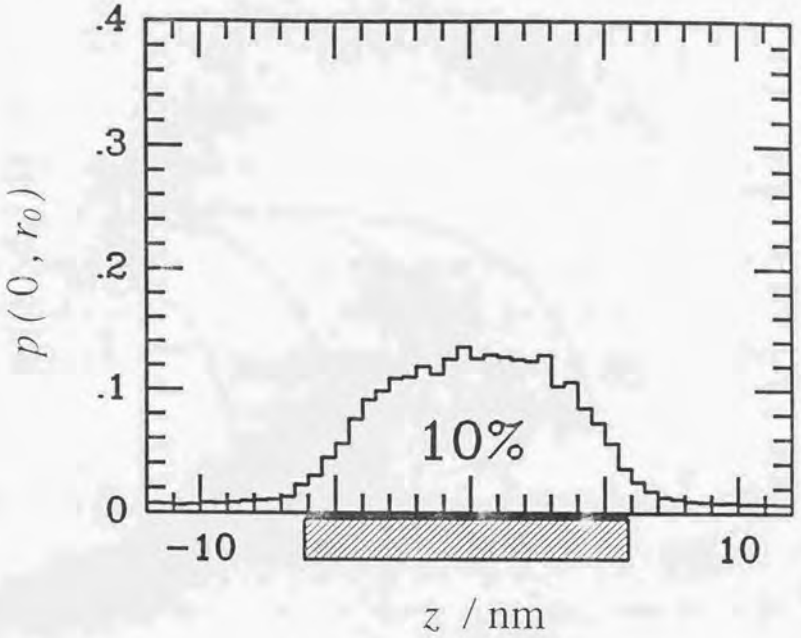

Fig.3-4-6 Counterion distribution near the polyion (r_0 = 1nm).
ξ =1, T = 298 K, l = 12nm, N = 16, c_P = 3.0mM c_R = 48mM.

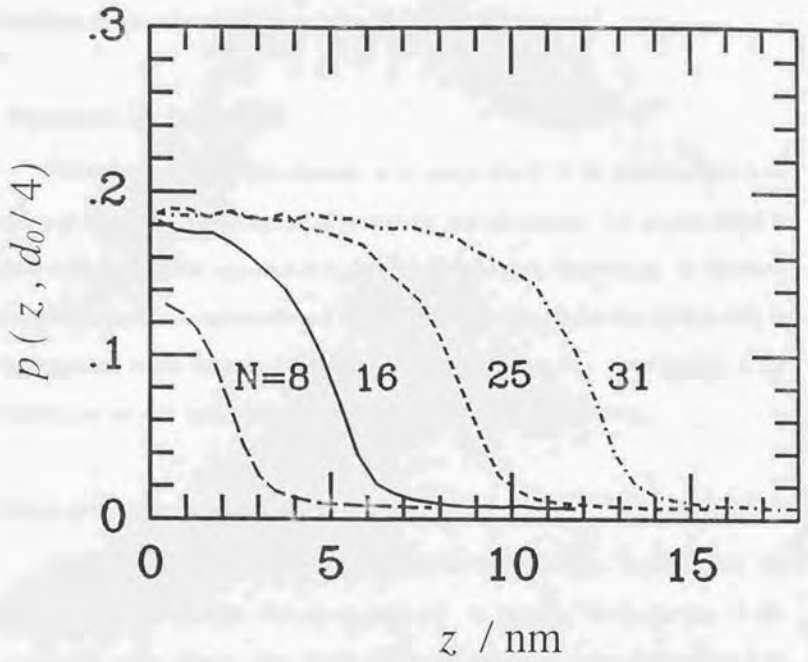

Fig.3-4-7 Counterion distribution at the polyion end . $\xi = 1$, $T = 298$ K
$l = 6$nm (N =8), 12nm (N =16), 18nm (N =25), 24nm (N =31).

However, if the length along z-axis is scaled by the Debye length d_0, the four curves agree with each other (Fig.3-4-8). Fig.3-4-9 shows the radial distribution of the counterions. The end effect above is also seen.

Dependence on ξ parameter

The counter ion distribution depends on the charge density of the polyion. Fig.3-4-10 shows ξ dependence of the number of counterions near the polyion. The polyion length is fixed at 12 nm, then the separation b is changed. In this figure, the radius r_0 is chosen to be d_0 / 4 in order to avoid the effect of the concentration. The broken line in Fig.3-4-10 is the theoretical results from the Manning's model . It is seen that some amount of the counterions are still associated near the polyion, even if ξ is below unity.

Effect of boundary condition

Boundary condition is very important factor for the simulations. In this section, the periodic boundary condition was always imposed. In principle, the image ions in the surrounding replica cells are taken into account for calculating the energy difference ΔU in the Metropolis scheme. Fig.3-4-11 shows the potentials from the simulations with and without image cells. The potential without image cells is higher than that with the image calls near the polyion.

Effect of temperature

Simulations were carried out for 298K. However, in order to check the accuracy of the calculation, several simulations for different temperatures were carried out. Then the temperature dependence were found to agree with that from the Boltzmann distribution.

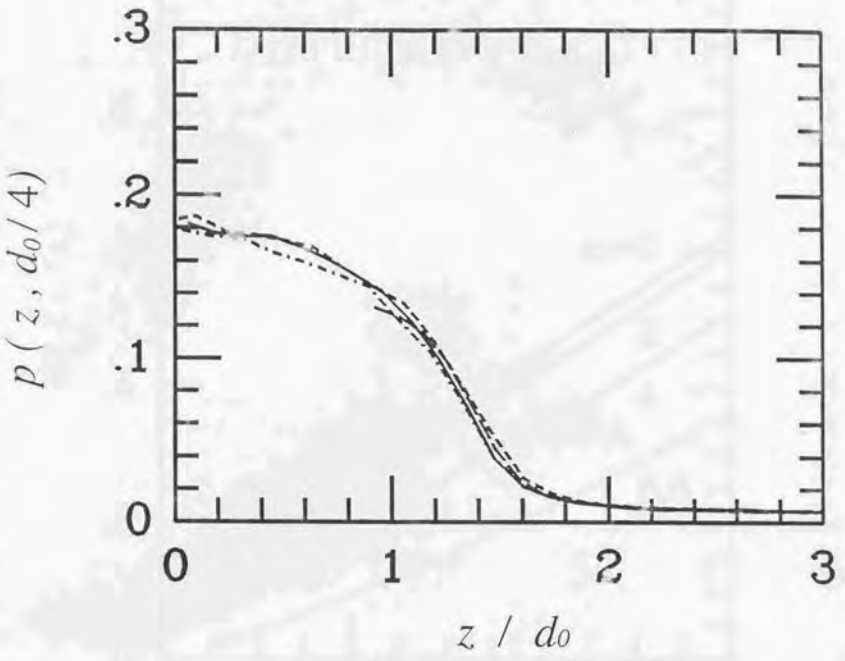

Fig.3-4-8 Counterion distribution at the polyion end scaled by the Debye length d_0. $\xi = 1, T = 298$ K, $l = 6$nm (N =8), 12nm (N =16), 18nm (N =25), 24nm (N =31).

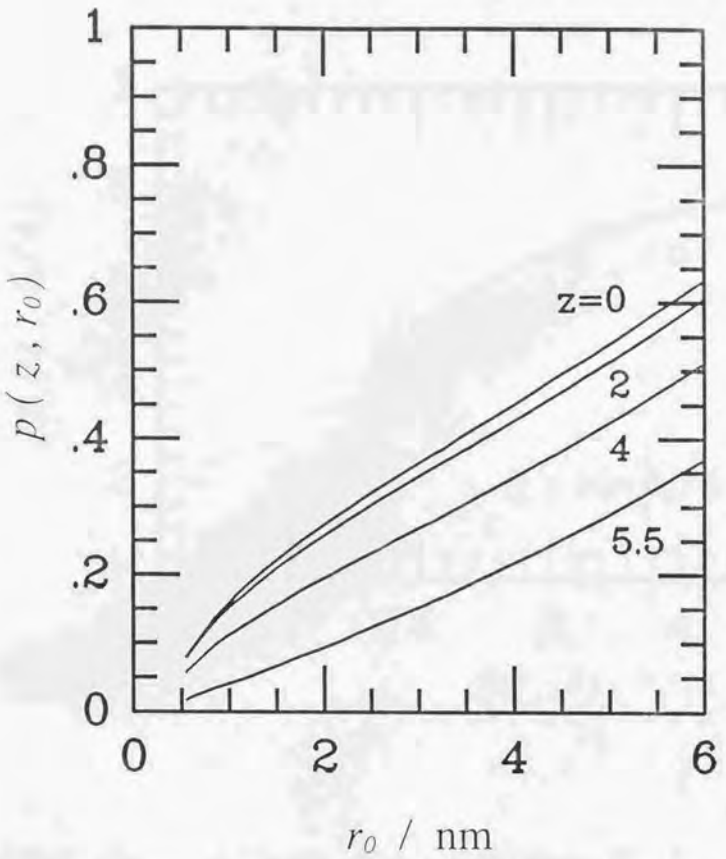

Fig.3-4-9 Integrated radial distribution of the counter ions.
$\xi = 1$, $T = 298$ K, $l = 12$nm, $N = 16$, $c_P = 3.0$mM $c_R = 48$mM.

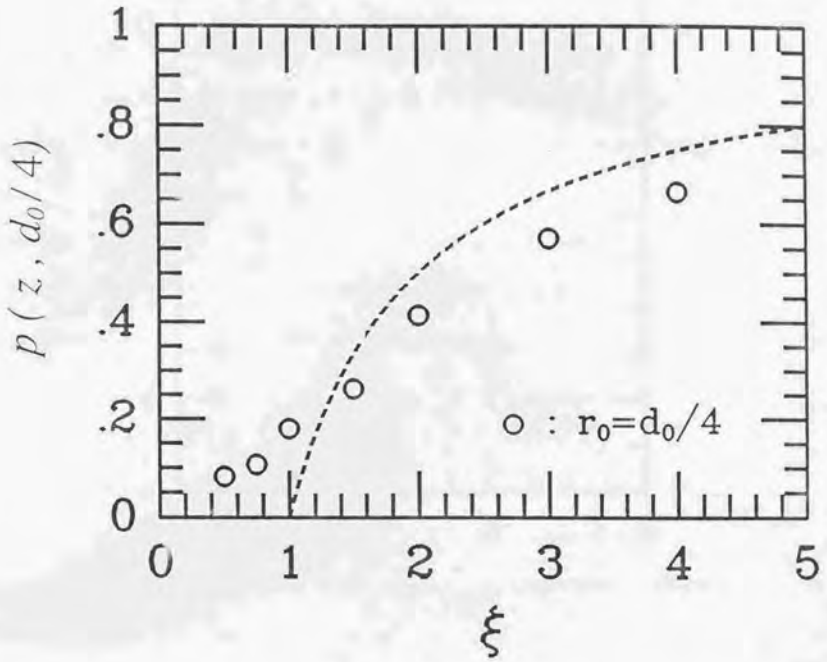

Fig.3-4-10 Polyion charge density ξ dependence of the number of counterions near the polyion. ○ : simulation, broken line : $1 - 1/\xi$. c_R = 48mM, T = 298 K.

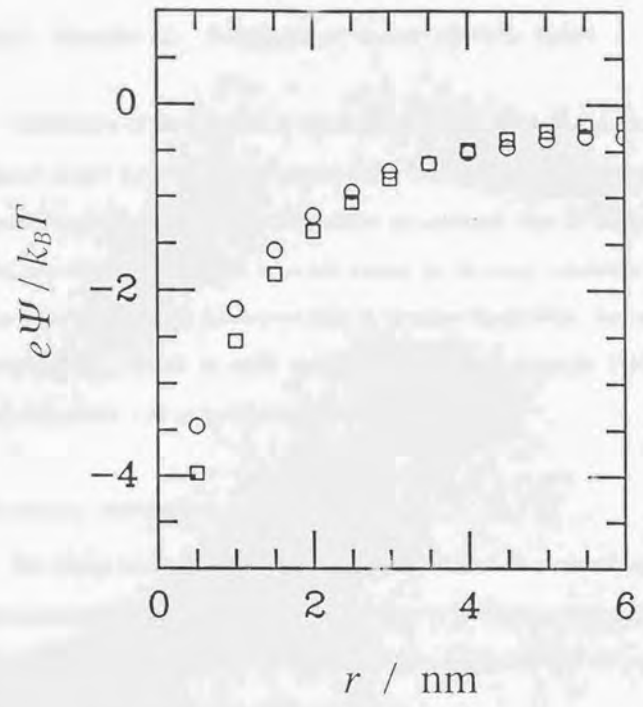

Fig.3-4-11 Effect of the boundary condition on the potential Ψ .
○ : simulation with replica cells, □: simulation without replica cells.
$\xi = 1$, $T = 298$ K, $l = 12$nm, $N = 16$, $c_P = 3.0$mM $c_R = 48$mM.

3.4.3 Results (2) Polarization under electric fields

Polarization of the counterions under an external electric field was simulated . The external electric field was applied parallel to the axis of the polyion. Periodic boundary conditions are imposed. In order to reproduce the stationary flow of the counterions, at least two image cells should be taken into account for the energy calculation (Fig.3-4-2). Since, the system under the external field is no more steady state, the maximum trial movement d_{max} should be small enough as discussed in chapter 2. The time step Δt was chosen to be 1.25 ps for the simulations in this section.

Counterion distribution

The counter ion distributions under the external electric field are shown in Fig.3-4-12. It is seen that the counter ions near the polyion shift in the direction of the field. Fig.3-4-13 shows the field strength dependence of the counterion distribution near the polyion surface. The vertical axis is the amount of the counter ions :

$$P(z, r_0) = \int_{z-\frac{b}{2}}^{z+\frac{b}{2}} \int_{0}^{r_0} \rho(z, r)\, 2\pi r\, dr\, dz \qquad (5)$$

The percentages in this figure are calculated as:

$$x = \frac{1}{N} \int_{-l/2}^{l/2} p(z, r_0)\, dz \qquad (6)$$

where, N is the number of counter ions in the unit cell, and the integral corresponds to the

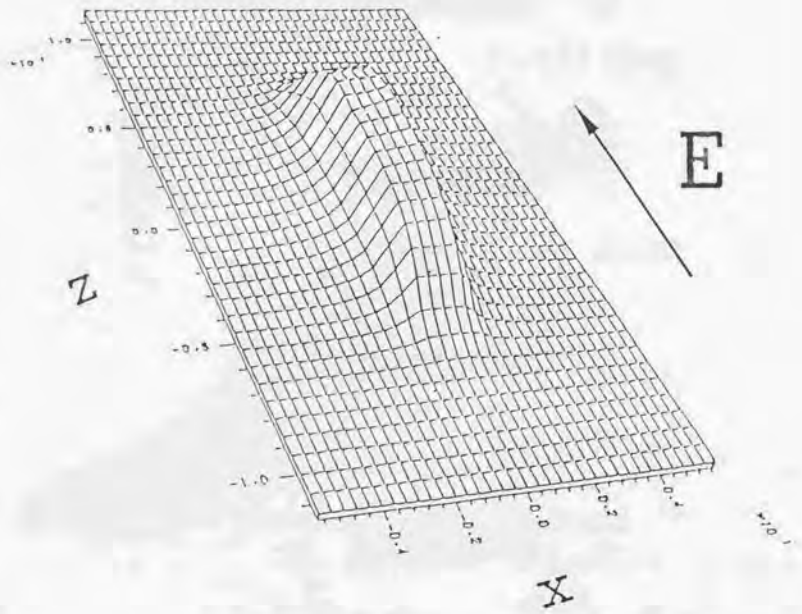

Fig.3-4-12 Counterion density under the external electric field E .
$\xi = 1$, $T = 298$ K, $l = 12$nm, $N = 16$, $c_P = 3.0$mM $c_R = 48$mM.

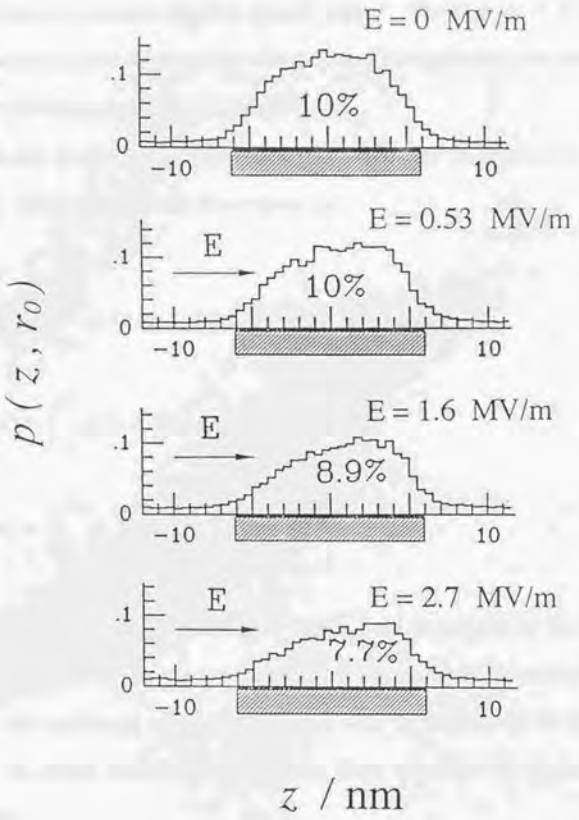

Fig.3-4-13 Effect of the external field E on the counterion distribution near the polyion. $\xi = 1$, $T = 298$ K, $l = 12$nm, $N = 16$, $c_P = 3.0$mM $c_R = 48$mM.

number of ions in a cylinder of radius r_0 and height l. The decrease of the percentage suggests that the counterions escape form the polyion. This can be said to be the Wien effect, because the field strength E is the order of 10^6 V/m.

The radial distribution of the counterions are shown in Fig.3-4-14, Fig.3-4-15, Fig.3-4-16. The vertical axes of these figures are :

$$q_T^{'}(c) = \int_{-l/2}^{-l/2} \rho(z, r)\, 2\pi r\, dz \tag{7}$$

$$q_A^{'}(r) = \int_{-l/2}^{l/2} \rho(z, r)\, 2\pi r\, dz \tag{8}$$

$$q_B^{'}(r) = \int_{-l/2}^{-l/2} + \int_{l/2}^{l/2} \rho(z, r)\, 2\pi r\, dz \tag{9}$$

Fig.3-4-14 shows that the counterions escape form the polyion by the effect of the external field. Fig.3-4-15 also shows the similar tendency. On the other hand, Fig.3-4-16 shows that the number of counter ions increase with the increase of the field strength. Therefore, the escape from the polyion results from their flow in the direction of the external field.

The flow of the counter ions can be predicted from the potential curves (Fig.3-4-17 and Fig.3-4-18). Fig.3-4-17 shows the potential curves on the surface of the polyion. The well is inclined and the threshold becomes lower under the external fields . This causes the ion flow in the direction of the applied field. Fig.3-4-18 shows the potential curves away from the polyion. The potential well is very shallow even at low field strength. Then, under the strong fields, the well-like potentials vanishes.

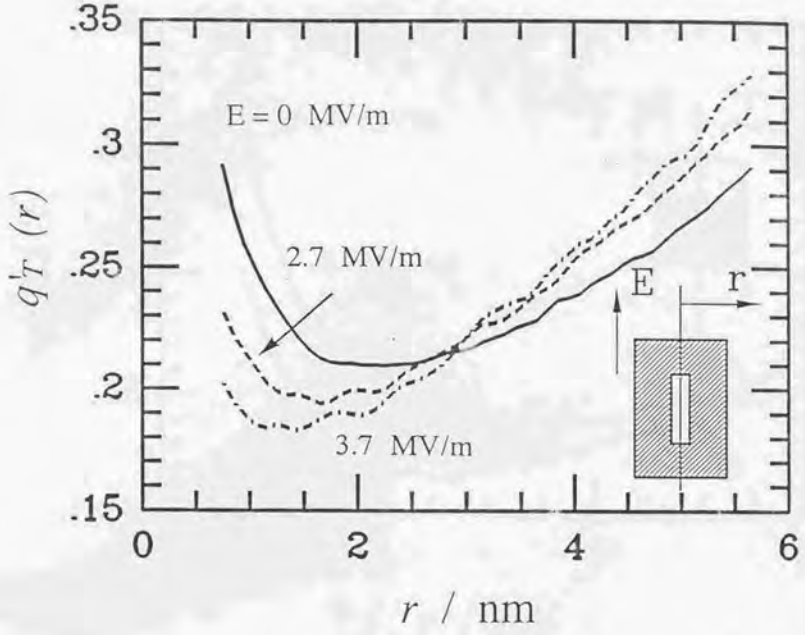

Fig.3-4-14 Effect of the external field E on the radial distribution of the counterion. $\xi = 1$, $T = 298$ K, $l = 12$nm, $N = 16$, $c_P = 3.0$mM $c_R = 48$mM.

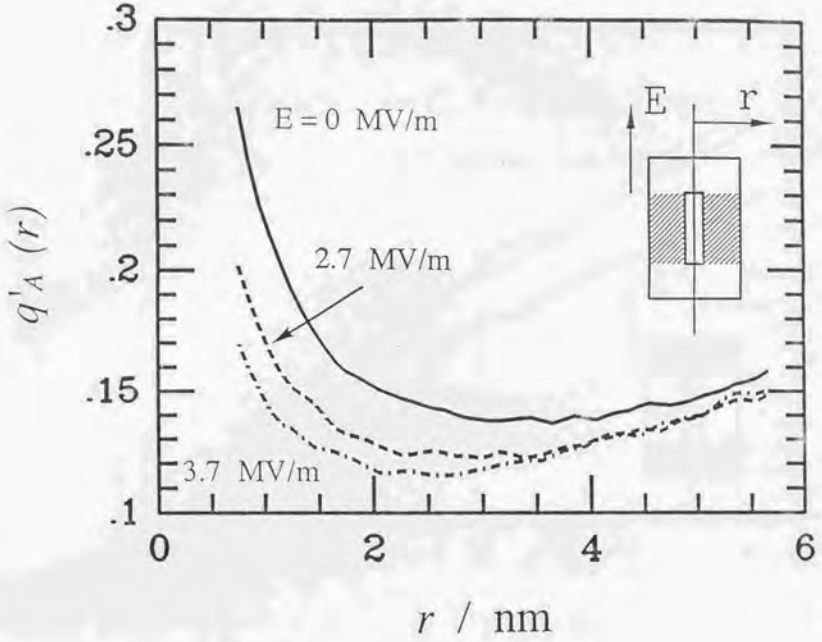

Fig.3-4-15 Effect of the external field E on the radial distribution of the counterion. $\xi = 1$, $T = 298$ K, $l = 12$nm, $N = 16$, $c_P = 3.0$mM $c_R = 48$mM.

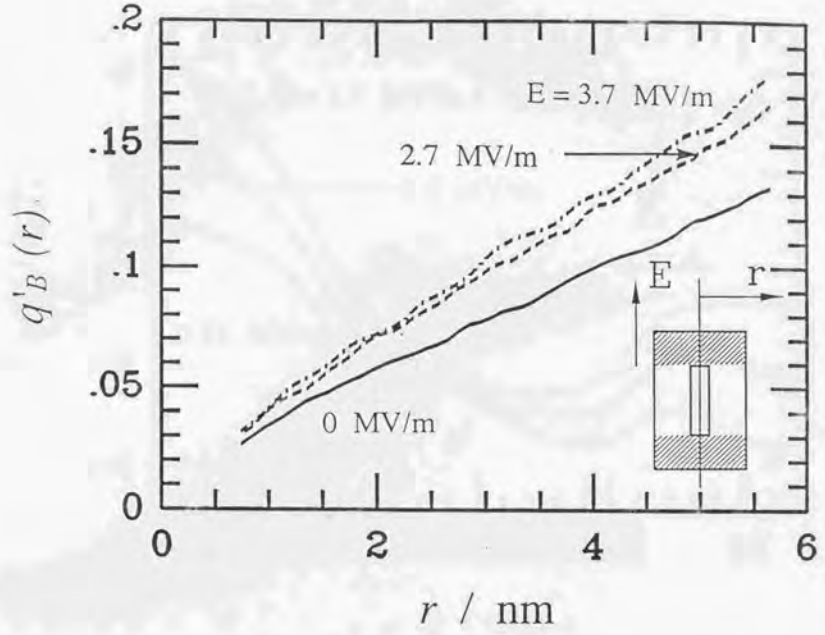

Fig.3-4-16 Effect of external field E on the radial distribution of the counterion. $\xi = 1$, $T = 298$ K, $l = 12$nm, $N = 16$, $c_P = 3.0$mM $c_R = 48$mM.

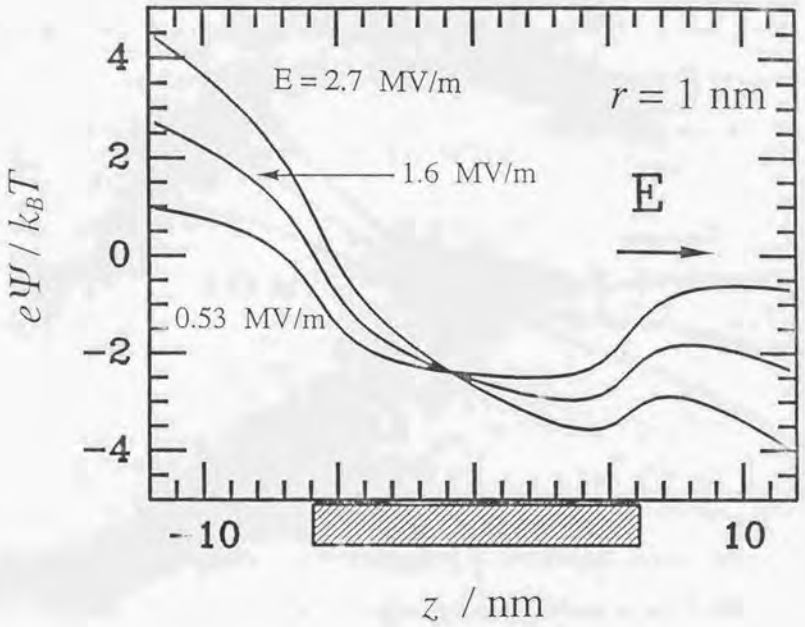

Fig.3-4-17 Effect of external field E on the potential Ψ near the polyion. $\xi = 1$, $T = 298$ K, $l = 12$nm, $N = 16$, $c_P = 3.0$mM $c_R = 48$mM.

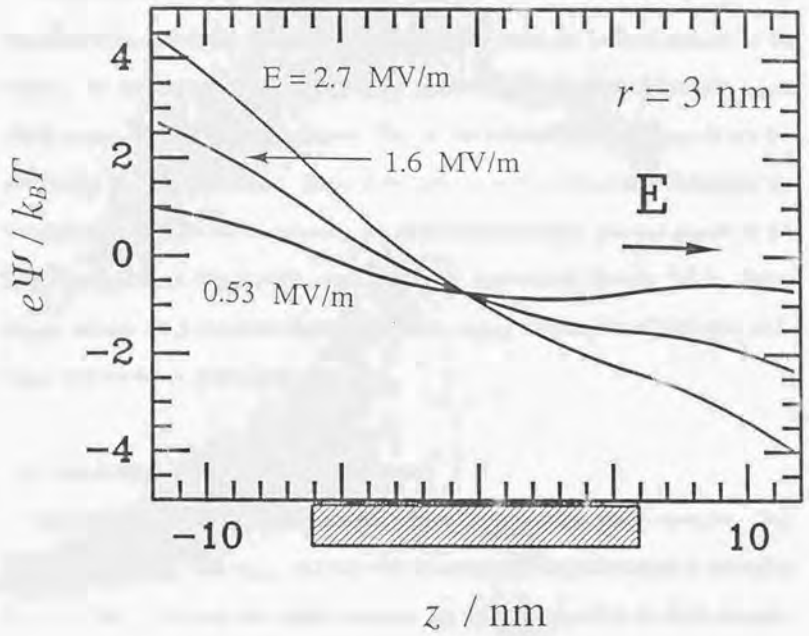

Fig.3-4-18 Effect of external field E on the potential Ψ distant from the polyion. $\xi = 1$, $T = 298$ K, $l = 12$nm, $N = 16$, $c_P = 3.0$mM $c_R = 48$mM.

Induced dipole moment

As discussed above, the polarization of the counterions is successfully reproduced by the Monte Carlo simulation. However it is difficult to define the induced moment of the polyion. In experimental studies, the induced dipole moment are obtained from the torque which causes the rotation of the polyion. That is, the induced dipole moment is not the polarization of all the counterion. Since it is difficult in the simulation to distinguish the counterions responsible for the rotation , we divide the counterions into two groups for the sake of convenience (Fig.3-4-19) according to the conventional theories [2,3,4]. Then, m_{asso} denotes the polarization of associated ions , m_{free} denotes that of free ions, and m_{totl} denotes that of all the ions.

***E* dependence of induced dipole moment**

Fig.3-4-20 shows the field strength dependence of the induced dipole moments. The dipole moment m_{totl} and m_{free} increase with the increase of the field strength in the region $E < 7$ MV/m . However ,the dipole moments are not proportional to the field strength. Then, if m is written as $m = \alpha E$. However ,the dipole moments from the simulations are not proportional to the field strength.

These dipole moments, m_{totl} and m_{free} saturate at about E = 7 MV/m , and then they decrease with the increase of the field strength. Such decreases at high field strengths are caused by the flow of the counter ions as discussed above. Since the values of these field strengths are the order of 10^6 V/m , the decrease of the dipole moments can be said to be the Wien effect. This reduction is results form the flow of the counter ions as mentioned above. The dipole moment will be zero if the counter ions flow at constant velocity.

On the other hand, the dipole moment m_{asso} and m_{av} do not decrease in the same

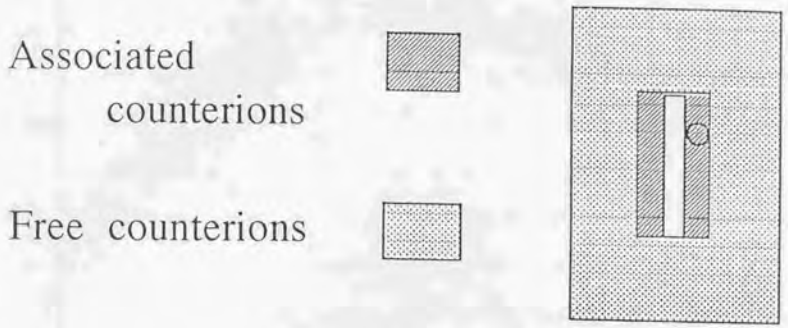

Fig.3-4-19 Definition of the associated counterion and the free counterion.

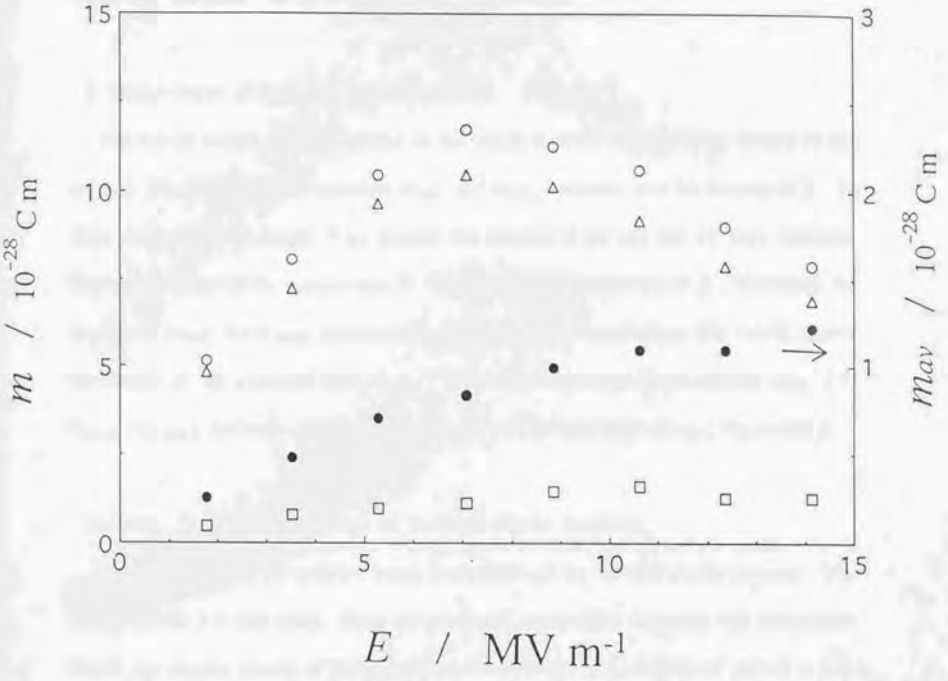

Fig.3-4-20 Field strength E dependence of the induced dipole moments. ○: m_{totl}, △: m_{free}, □: m_{asso}, ●: m_{av} (= m_{asso} / n_{asso}) ξ = 1, T = 298 K, l = 12nm, N = 16, c_P = 3.0mM. c_R = 48mM.

range. The contribution of the associated counter ions is defined as $m_{av} = m_{asso} / n_{asso}$. Then, m_{av} increases with the increase of the field strength.

ξ dependence of induced dipole moment

Fig.3-4-21 shows the dependence of the dipole moment on the charge density of the polyion. The induced dipole moments m_{totl} and m_{asso} increase with the increase of ξ. In these simulations, the length of the polyion and the size of the unit cell are kept constant. Then, the number of the counter ions N increases with the increase of ξ. Therefore, the increase of m_{totl} and m_{asso} are caused by the number the counter ions. Fig.3-4-22 shows the increase of the associated ions n_{asso}. However the average dipole moment m_{av} (= m_{asso} / n_{asso}) decreases due to the repulsion between the associated ions (Fig.3-4-23).

Polyion length dependence of induced dipole moment

Fig.3-4-24 shows the polyion length dependence of the induced dipole moment . The charge density ξ is kept unity. Since the number of counter ions increases with the polyion length, the number density of the counter ions will change if the volume of the cell is kept constant. In order to clarify the effect of the density, we carried out two series of simulations. The one is the simulation of a constant volume and the other is those of constant density. In the latter case, the volume of the system is changed by stretching the cell in the direction of the field.

The dipole moments, m_{asso} and m_{totl} , are found to be proportional to the third power of the polyion length , if the density of the counter ions is kept constant. This result agrees to that from electro-optical measurement. Even if the density of the ions is not kept constant, the moment m_{asso} is also proportional to the third power of the polyion length. This implies

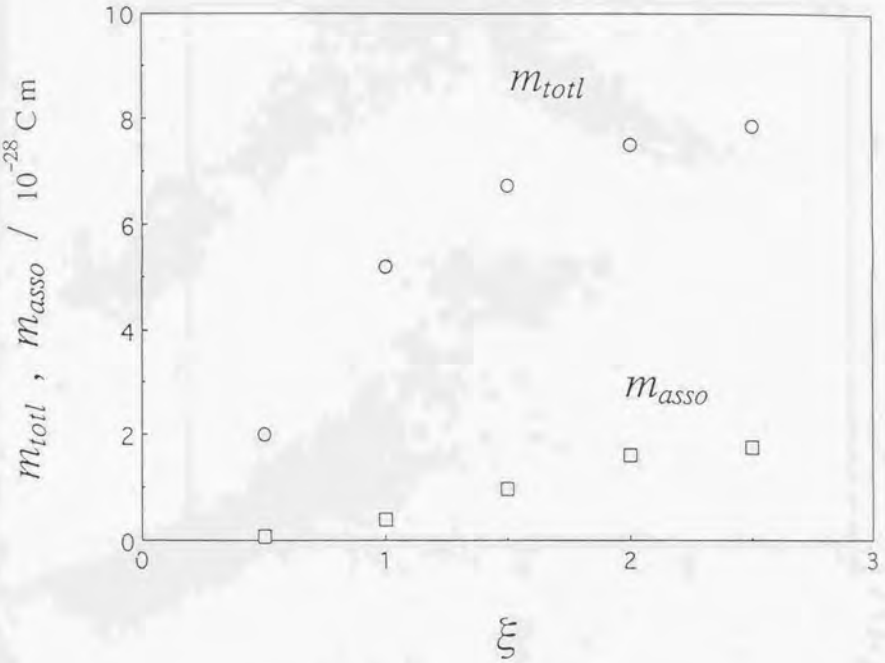

Fig.3-4-21 Polyion charge density ξ dependence of the induced dipole moments. ○: m_{totl} , □ : m_{asso} T = 298 K, l = 12nm, c_R = 48mM.

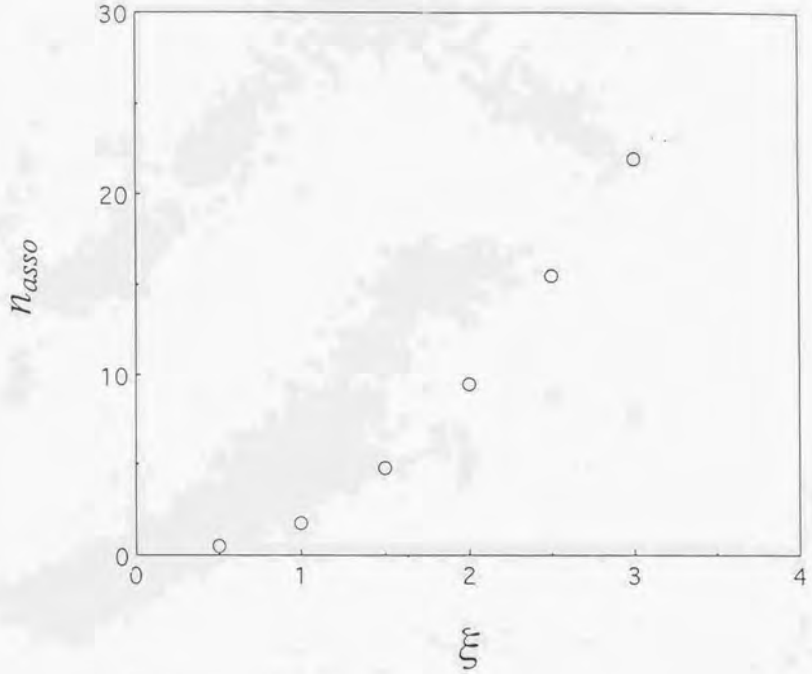

Fig.3-4-22 Polyion charge density ξ dependence of the number of associated ions n_{asso}. $T = 298$ K, $l = 12$nm, $c_R = 48$mM.

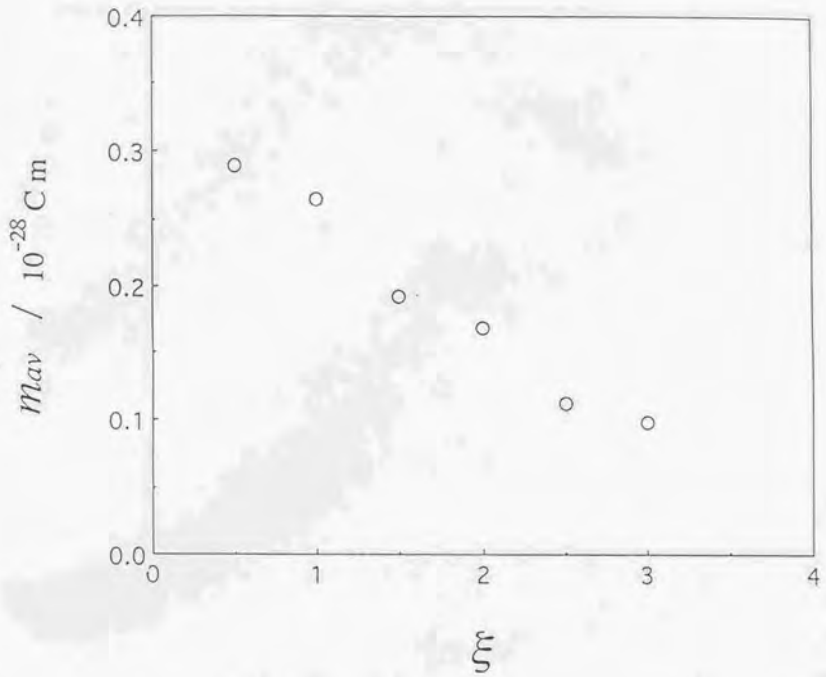

Fig.3-4-23 Polyion charge density ξ dependence of the average dipole moment m_{av} (= m_{asso} / n_{asso}) T = 298 K, l = 12nm, c_R = 48mM.

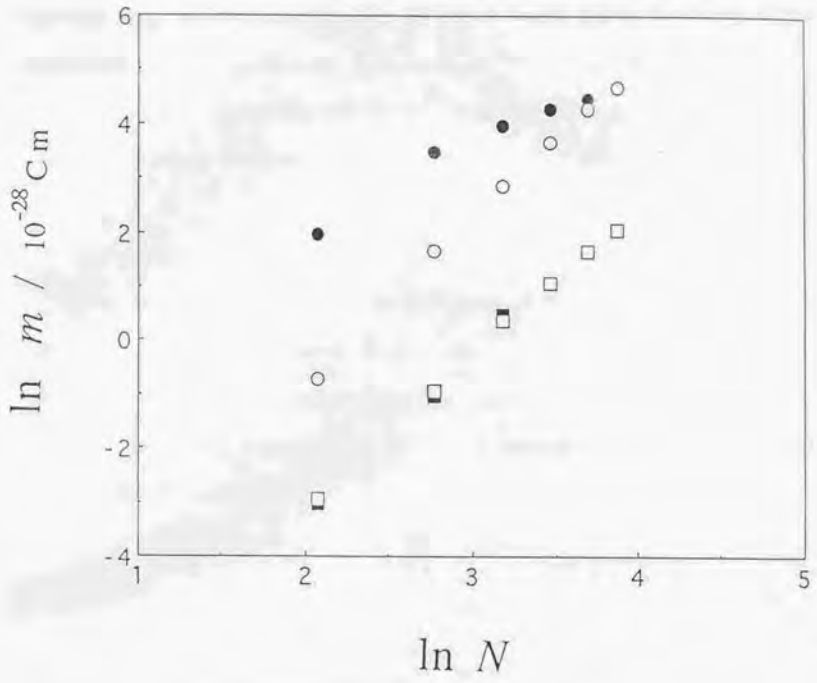

Fig.3-4-24 Polyion length dependence of the induced dipole moments.
○: m_{totl} ,□ : m_{asso} for constant counterion concentration (c_R = 48mM).
●: m_{totl} ,■ : m_{asso} for constant polyion concentration. (c_P = 3.0mM).
ξ =1, T = 298K. l = 6nm (N =8), 12nm (N =16), 18nm (N =25),
24nm (N =31), 30nm (N =41), 36nm(N =50).

that the environments of the associate ions does not much depend on the total density. However, m_{totl} is almost proportional to the polyion length, that is, the density of the counter ions.

3.4.4 Results (3) Relaxation times of polarization

The relaxation time of the polarization was successfully obtained from the Monte Carlo simulation. Since the relaxation time of mono-disperse DNA fragments were measured by Porschke, simulation for a model DNA fragment was carried out , and the polarization of all the counterions m_{totl} were analyzed and discussed.

Time evolution of polarization

Fig.3-4-25 shows the transient of the polarization of the simulation . Since the DNA fragment of 64 base pairs is considered, the degree of polymerization N is 128. The field strength is 7.0 MV / m . The counterions were considered as Na^+ ions. This transient curve was obtained from the accumulation of 100 runs. It took about 50 hours by our work station HP9000-715 of 31 Mflops.

The transient curve can be fitted by a single exponential.

$$m = m_0 (1 - exp (- t / \tau)) \qquad (10)$$

Then the relaxation time is defined as $-\tau$. In the case of Fig.3-4-25, the relaxation time τ was obtained as 3.6 ns. This single exponential curves can be analyzed by assuming the motion of the ions as the harmonic oscillation :

$$\frac{d^2x}{dt^2} + \beta \frac{dx}{dt} + \omega^2 x = F \qquad (11)$$

where, x is the displacement of the ions, F is the external force, the second term represents the frictional force, and the last term represent the force of restitution proportional to the

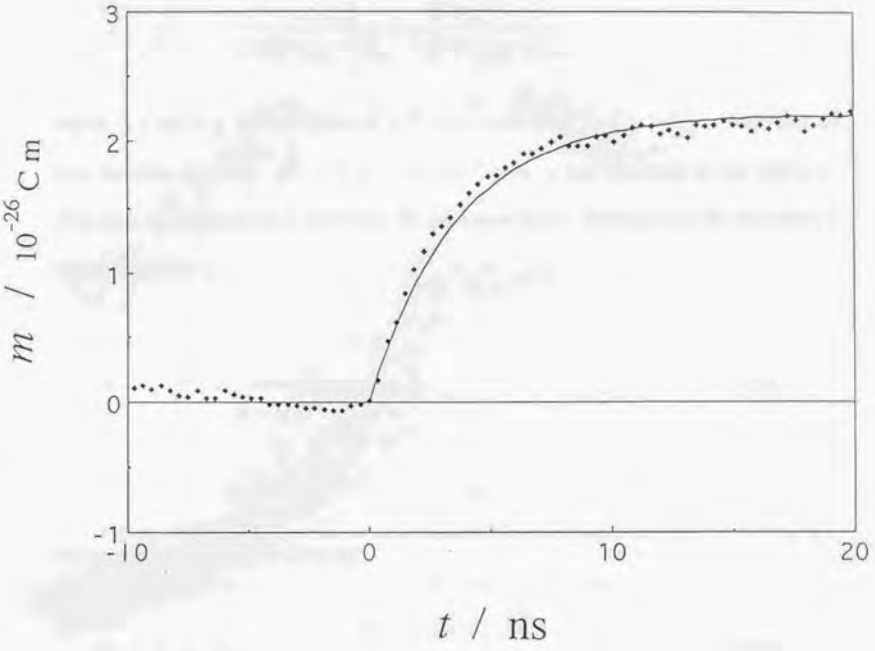

Fig.3-4-25 Time evolution of the induced dipole moment of 64 base-pair DNA. The external field is applied at t =0. E = 7.1 MV/m , ξ =4.1, T = 298K, l = 24nm, c_P = 0.32mM, c_R = 41 mM .

displacement. The solution of this equation is known:

$$x = \frac{F}{\lambda_1 \lambda_2} + \frac{F \exp(\lambda_1 t)}{\lambda_1 \exp(\lambda_1 - \lambda_2)} + \frac{F \exp(\lambda_2 t)}{\lambda_2 \exp(\lambda_2 - \lambda_1)} \qquad (12)$$

where, λ_1 and λ_2 is the solution of $\lambda^2 + \beta\lambda + \omega^2\lambda = F$, $\lambda_1 > \lambda_2$. Assuming the over dumping process, $\beta^2 > 4\omega^2$, the third term is not dominant in the equation. Therefore, if the third term is neglected, the relaxation time τ obtained from the simulation is written by β and ω :

$$\tau = \frac{1}{\lambda_1} = \frac{2}{\beta - \sqrt{\beta^2 - 4\omega^2}} \qquad (13)$$

The spring constant ω^2 is given by :

$$\omega^2 = F / x(\infty) \qquad (14)$$

Then friction coefficient β , which reflect the dynamic properties , is written as:

$$\beta = 1/\tau + \omega^2 \tau \qquad (15)$$

Thus, the spring constant ω^2 and the friction coefficient β are calculated from the relaxation time τ.

Polyion length dependence of τ

Table 3-4-1 shows the dependence of the degree of polymerization. The relaxation time τ was found to increase with the increase of the degree of polymerization. This is caused by the increase of the displacement of the counter ions, because the polyion length which is proportional to N. The increase of the displacement reflected the decrease of the spring constant ω^2. The friction constant β was found to be independent of the degree of polymerization N. This implies that the environment of around a counter ion does not change.

Dielectric constant dependence of τ

Table 3-4-2 shows the dependence on the dielectric constant D of the solvents. The relaxation time was found to decrease with the decrease of the dielectric constant. The steady state value of the dipole moments m_{totl} and m_{asso} also decrease with the decrease of the dielectric constant. Therefore, the decrease of the relaxation time is caused by the decrease of the displacement of counter ions due to the strong repulsive interaction between the counter ions. The decrease of the dielectric constant is equivalent to the decrease of the temperature.

Field strength dependence of τ

Table 3-4-3 shows the dependence of the relaxation time on the field strength E. The relaxation time τ becomes shorter with the increase of the field strength E. The spring constant ω^2 in eq(14) increases with the increase of E. Therefore, the decrease of τ results from eq(13).

Table 3-4-1 DNA length dependence of the relaxation time τ.
T = 298K, E = 10.6 MV/m, c_R = 41 mM (in the unit of nucleotide residues).

Nucleotide residues, N	Base pairs	τ / ns
64	32	0.73
96	48	1.9
128	64	2.7

Table 3-4-2 Effect of solvent dielectric constant ε on relaxation time τ of 64 nucleotide residues DNA. T=298K, E=10.6 MV/m, c_R =41mM.

ε	τ / ns
78.3	0.833
20.0	0.157

Table 3-4-3 Field strength E dependence of the relaxation time τ of the 128 nucleotide residues DNA (64 base pairs). T = 298K, c_R = 41 mM (in the unit of nucleotide rediues).

E / MVm^{-1}	τ / ns
3.5	5.0
7.0	3.6
10.6	2.7

Concentration dependence of τ

Table 3-4-4 shows the dependence of τ on the concentration of the solutions. The relaxation time τ becomes slower with the increase of the field strength E. The spring constant ω^2 in eq(14) increases with the increase of the concentration . Therefore, the decrease of τ results from eq(13).

Effect of added salt

Finally, the effect of added salts was also investigated. This is important for comparing to the experimental data, because a salt is added in almost measurements including Porschke's one. Table 3-4-5 shows that the relaxation time increases if the salt is added.

Table 3-4-4 Concentration c_R dependence of the relaxation time τ of the 128 nucleotide residues DNA (64 base pairs). T = 298K, E = 7.0 MV/m . (c_R is given in the unit of nucleotide residues)

c_R / mM	τ / ns
164.0	2.6
41.0	3.6
10.3	4.8

Table 3-4-5 Effect of the added salt on the relaxation time τ of the 64 nucleotide residues DNA (32 base pairs). T = 298K, E = 10.6 MV/m. c_R = 41mM (in the unit of nucleotide residues). NaCl is added so that the concentration of the total Na^+ is 61.5mM.

	τ / ns
Added salt	1.1
Without salt	0.73

3.4.5 Discussion

The polarization of the counterions was obtained by the Monte Carlo method [1]. This was the first simulation work which reproduced the counterion polarization. The simulated polarization can be compared to the induced dipole moments in experiments. However, there have been various definitions of the induced dipole moment . Schwartz [2, 3, 4] proposed that the longitudinal movement of 'bound ions' on the surface of the polyion is the origin of the induced dipole moments. The polarization of the 'associated ion' in this work may correspond to the model. However, definition of 'bound ions' and 'associated ions' are vague and arbitrary . Rau and Charney [5, 6] calculated the induced dipole moment as the polarization of the Debye Huckel distribution of the counter ions. The results in this thesis may correspond to those by Rau and Charney.

The relaxation times of the polarization were obtained in the Monte Carlo simulation[7]. The slow induced dipole moment model has been proposed in order to explain experimental data. The results in this section implies that the slow induced moment can be realized in a simple system which consists of coulombic interacting ions. Since the relaxation times were the order of 10^{-9} second, the speed of the Monte Carlo calculation was made the best use of. Table 3-4-6 shows comparison with the experiments of Porschke [8]. The simulated relaxation time was found to be rather shorter than that from Porschke's experiment. This may results from the difference of the concentration. The concentration of Porschke's measurement is about 1 / 500 of our simulation, and the relaxation time was found to becomes longer with the decrease of the concentration. Simulation for such dilute solution is desirable for comparison with experiments, however it is future subject because of the computation time. The definition of the induced dipole moment is also different even if simulation for dilute solutions are carried out. The best way for comparison to the experiment will be to simulate the rotation of the polyion due to the polarization of the counterions as discussed section 3.5.

Table 3-4-6 Comparison with experimental results.

	Nucleotide residues	c_R / mM	E / MVm^{-1}	τ / ns
Monte Carlo Simulation	128	10.3	7.0	4.8
Experiment (Porschke)	152	0.02	6.88	16.6

References

1) Yoshida,M.,Kikuchi,K., Maekawa,T., and Watanabe,H. *J.Phys. Chem.* **96**, 2365 (1992)

2) Schwarz,G. *Z.Phys.* **145**, 563 (1956)

3) Schwarz,G. *Z.Phys.Chem.* **19**, 286 (1959)

4) Schwarz,G. *J.Phys.Chem.* **66**, 2636 (1962)

5) Rau,D.C and Charney,E. *Biophys.Chem.* **14**,1 (1981)

6) Rau,D.C and Charney,E. *Mocromolecules* **16**, 1653 (1983)

7) Yoshida,M., and Kikuchi,K.*J.Phys. Chem.* **98**, 10303(1994)

8) Porschke, D. *Biophysical Chemistry* **22**, 237 (1985)

3.5 Rotation of polyion coupled with counterion polarization

The origin of the induced dipole moment of polyelectrolytes that is strong enough to orient the polyion is still poorly understood even if simple models are assumed for the geometry of the polyions. In many theoretical studies, *ad hoc* approximations have been postulated such that counterions are classified into " free " and " bound " ions, only the latter contributing to the induced moment.

In the previous sections we have determined amplitudes and relaxation times of the counterion polarization by accounting for only small ion distribution around a fixed polyion. While extensive calculations with more realistic models may be needed for comparison with experiment, our greatest concern throughout this thesis is whether simulations without constraining the polyion at a fixed alignment reproduce its orientation. Counterions in the immediate vicinity of the polyion are so firmly bound to polyion that their contribution to the induced dipole moment is small. On the other hand counterions far away from the polyion are easily polarized and even stripped from the electrostatic influence of the polyion at high electric field. Then we may well wonder whether the diffuse ion cloud around the polyion when polarized under the influence of an external field can indeed exert a torque strong enough to orient the polyion. In view of the fact that the counterion polarization processes in an applied electric field is measured experimentally *via* the orientation of the polyelectrolyte molecule, simulation of the coupled rotational and ion atmosphere dynamics of a polyelectrolyte might be most helpful in the interpretation of the electric polarizability data. In this section, we attempt to reproduce orientation dynamics of polyelectrolytes by computer simulation.

3.5.1 Model and Simulation

The polyion is modeled on a 64 base-pair DNA fragment as an impenetrable cylinder of radius 1.0 nm with 128 negative charges spaced at 0.17 nm intervals along its axis. The cylinder is extended 0.17nm beyond the terminal charges at both ends The hydrated univalent counterions are modeled on sodium ions as hard spheres of radius 0.15nm. The solvent is treated as a dielectric continuum with relative permittivity of pure water at 298K, $\varepsilon = 78.3$ and no salt added. The MC cell is a rectangular parallelepiped with squared base of side length 12nm and of height 36nm and the center of the polyion is fixed at the center of MC cell leading to a DNA concentration of 41mmol of nucleotide residues / dm^3. An electric field is applied along the height of the cell and the angle q specifying the orientation of the polyion rod is defined in Fig.3-5-1.

Periodic boundary conditions are imposed at each face of the MC cell. The energy of configurations is calculated as a sum of interactions of each counterion in the MC cell with all the other counterions and the polyion charges in the cell and two image cells adjacent along the direction of the electric field plus interactions of the ions with the applied electric field. Polyion-polyion interactions between the adjacent cells are neglected.

0.1nm is chosen as the size of the maximum allowed displacement d_{max} of counterions along each coordinate direction. The time interval for the simulation Δt is fixed as 1.25ps by the relation:

$$d_{max}{}^2 = 6D\Delta t \qquad (1)$$

using the diffusion coefficient of a sodium ion in bulk water $D = 1.33 \cdot 10^{-9}$ m^2s^{-2} . The maximum allowed rotation angle for polyion $\Delta\theta_{max}$ is somewhat arbitrarily chosen as 1.0 degree because our primary concern here is to test the feasibility of the simulation. The rotatory diffusion coefficient for the polyion D_R calculated by the relation:

$$\Delta\theta_{max}{}^{2} = 6D_R\Delta t \qquad (2)$$

using Δt =1.25 ps is about ten times larger than that expected for the dimension of the polyion cylinder from hydrodynamics.

Initially the polyion is directed 5 degrees off the direction of the applied field. The distribution of counterions are equilibrated. At $t = 0$, an electric field E of 7.0 MV/m is applied. Then the angle θ is followed as a function of time t and averaged over 300 trajectories.

3.5.2 Results

Fig.3-5-2 shows the results of the simulation. Relaxation of q from its initial value 5 degree to an equilibrium value is observed indicating that the orientation of the polyion is reproduced by the simulation.

3.5.3 Discussion

Although we used a rather restrictive model, we have shown that the orientation dynamics of polyelectrolytes under the influence of an applied electric field can be studied by computer simulation. The approach eliminates the distinction between " free " and " bound " counterions often assumed in analytical studies. We view our work as a sound first attempt presumable leading to the clarification of the mechanism of the orientation of polyelectrolytes in an electric field. However, extensive calculations with more realistic models are necessary for comparison with experiment.

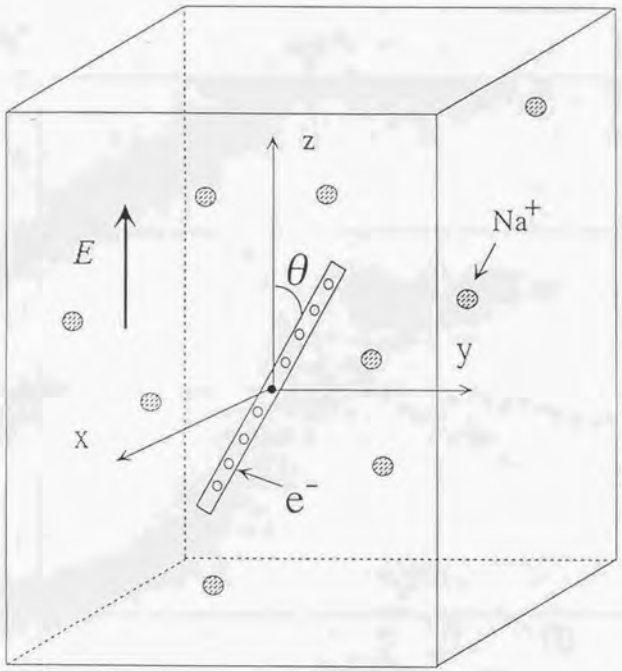

Fig.3-5-1 Model of the polyelectrolyte solution.

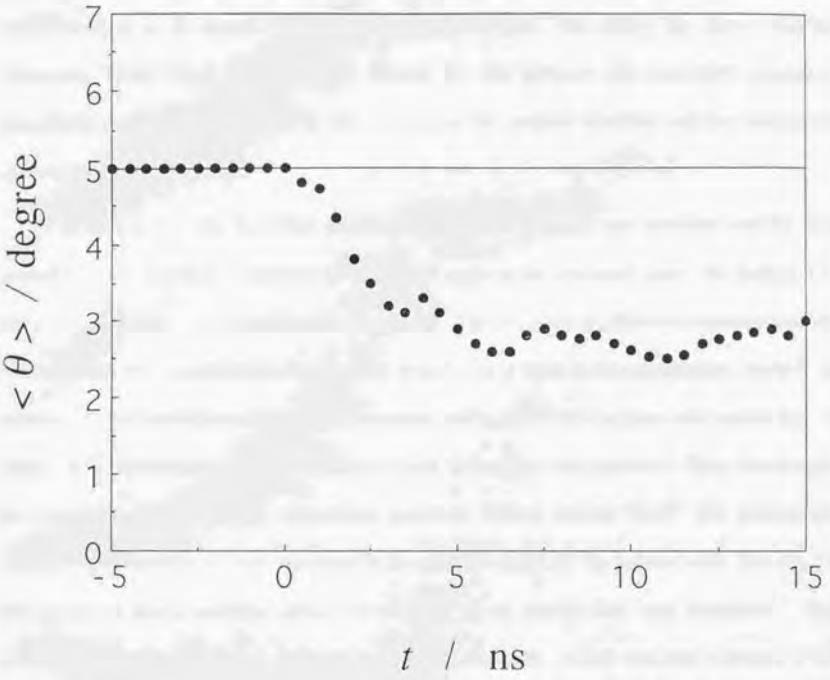

Fig.3-5-2 Rotational motion of the polyion coupled with the polarization of the counterions. Initial direction of the polyion: $\theta = 5$ degrees . The electric field applied in the direction of the z axis (t > 0). Polyion: 64 base pair DNA. Concentration of the polyion: $c_p = 0.32$ mM, T=298 K, $E = 7.0$ MV/m

4. Conclusion

The subject of this thesis has been to study the mechanism of the orientation of polyelectrolytes in an electric field by computer simulations. The author has shown that the Metropolis Monte Carlo is a powerful method for this purpose and developed simulation procedures step by step finally to be able to simulate the coupled rotational and ion atmosphere dynamics of a polyelectrolyte.

In section 3.1, the Brownian motion in a harmonic potential was simulated and the time evolution of its distribution function was found to agree to the analytical one[1]. In Section 3.2, diffusion of ions in NaCl solution was discussed. The diffusion coefficients were successfully obtained, and their concentration dependences were found to agree to the experimental results[2]. In section 3.3, the simulations of rotational Brownian motion of rod-like polyion were carried out. In Section 3.4, the behavior of the counterions around the polyion was simulated. First, we obtained the counterion distribution and electrostatic potentials without external field[3]. The electrostatic potential on the polyion surface was found to be constant except for the polyion ends. Second, the polarization of the counterions under the influence of an electric field was simulated[3]. The saturation and reduction of the polarization under strong fields , which has been observed in the experiments, was also reproduced by the simulation. The reason was found to be that counterions are stripped away from the polyions. Thus, the simulation can provide a microscopic explanation for the experimental results. Finally, relaxation times of counterion polarization were calculated[4]. The relaxation times were longer than the order of 10^{-9} second, the merit of Monte Carlo simulation of calculating fast was appreciated. Their dependences on the polyion length, the concentration, and the field strength were found to qualitatively agree to the experimental results[5]. In Section 3.5, the simulation of the coupled rotational and ion atmosphere dynamics of rod-like polyelectrolytes was carried out. This is a basis of simulations for the response of electro-optical

measurements.

Although most of the simulations performed in this thesis are preliminary and extensive calculations with more realistic models are needed for comparison with experiment, the author believes that his method can be of general use for studying dynamics of polymers and colloids in solution whose motion is usually described by diffusion equation.

In order to carry out simulations corresponding to the experiments, there are some subjects to be considered. First, simulations in this thesis were carried out for simple rod-like model molecules. More precise structure of the polyion should be considered , however it is not a difficult problem. In principle, the accuracy and computation time do not depend on the shape of the molecule. Second, simulations for more dilute solutions should be carried out, however it requires more computation time due to the increase of the fluctuations. Thus, improvement of algorithm may be needed for reducing computation time. Then, most of simulations in this thesis were carried out for salt free solutions, however in experimental approach polyelectrolytes have been studied in salt added solutions. In this case, the boundary conditions should be carefully introduced. Finally, the hydrodynamic interaction between ions should be considered in some cases. Algorithm for this interaction has been already developed[6].

While the author focused on the simulations for the response of electro-optical measurement, this simulation technique can also be applied for the study of colloid suspensions and polymer solutions.

References

1) Kikuchi,K., Yoshida,M., Maekawa,T., and Watanabe,H. *Chem.Phys.Lett.* **185**, 335 (1991)

2) Mills,R *Reviews of Pure and Applied Chemistry*

3) Yoshida,M.,Kikuchi,K., Maekawa,T., and Watanabe,H. *J.Phys. Chem.* **96**, 2365 (1992)

4) Yoshida,M., and Kikuchi,K.*J.Phys. Chem.* **98**, 10303(1994)

5) Porschke, D. *Biophysical Chemistry* **22**, 237 (1985)

6) Kikuchi,K., Yoshida,M., Maekawa,T., and Watanabe,H. *Chem.Phys.Lett.* **196**, 57 (1992)

Acknowledgments

The author is very grateful to Professor Kazuo Kikuchi, Professor Tsuneo Maekawa, and Professor Hiroshi Watanabe. Most of the works in this thesis have been done in cooperation with them. The author is also thankful to Dr. Hirokazu Toriumi for his helpful advice. The author is much obliged to Professor Ryo Hirasawa, Professor Toschitake Iwamoto, Dr. Takafumi Kitazawa, and Professor Daiichiro Sugimoto for their encouragement to complete this thesis.

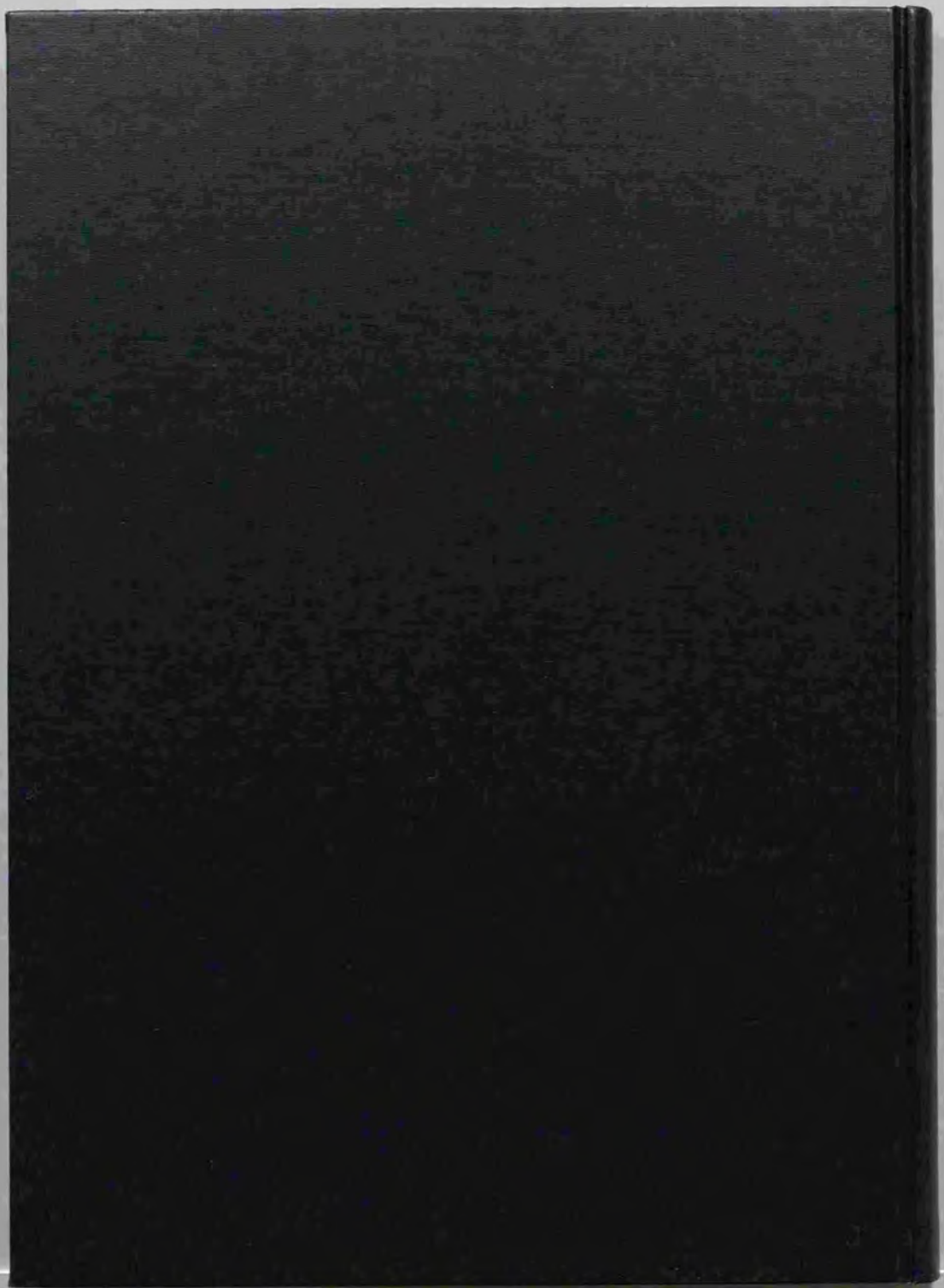

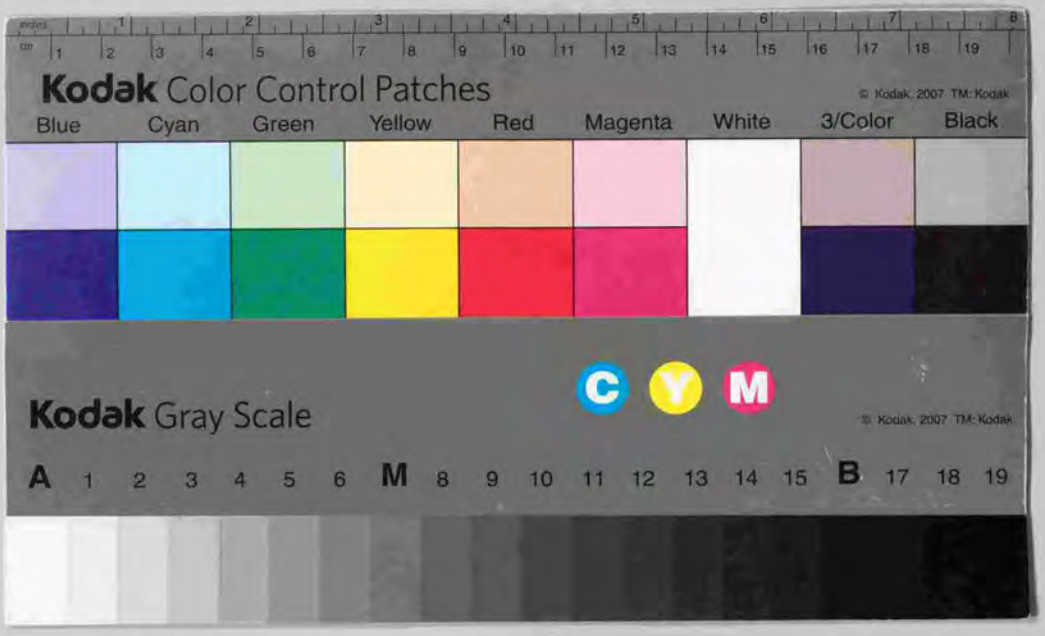
Kodak Color Control Patches
© Kodak, 2007 TM: Kodak
Blue
Cyan
Green
Yellow
Red
Magenta
White
3/Color
Black
Kodak Gray Scale
C
Y
M
© Kodak, 2007 TM: Kodak
A 1 2 3 4 5 6 M 8 9 10 11 12 13 14 15 B 17 18 19